Plant, Cell & Environment

WILEY

Plant, Cell & Environment

ORIGINAL ARTICLE

Drought-Induced Cyanogenesis in Sorghum (*Sorghum bicolor* L.): Genotypic Variation in Dhurrin Biosynthesis and Stress Response

Sri Cindhuri Katamreddy[1,2] | Jismon Jose[1,3] | Bommineni P. Reddy[1] | Kaliamoorthy Sivasakthi[1] | Hemalatha Sanivarapu[1] | Namita Dube[1] | Anil Gaddameedi[1] | Prasad Kodukula V.S.V[4] | Kalenahalli Yogendra[1] | Mahalingam Govindaraj[1,5] | Jana Kholova[1,6] | Swarup Roy Choudhury[3] | Polavarapu B. K. Kishor[2] | Padmakumar Varijakshapanicker[4] | Pooja B. Mathur[1,7] | Are A. Kumar[1] | Palakolanu Sudhakar Reddy[1]

[1]International Crops Research Institute for the Semi-Arid Tropics (ICRISAT), Hyderabad, Telangana, India | [2]Department of Genetics and Biotechnology, Osmania University, Hyderabad, Telangana, India | [3]Department of Biology, Indian Institute of Science Education and Research (IISER), Tirupati, Andhra Pradesh, India | [4]International Livestock Research Institute, Hyderabad, Telangana, India | [5]HarvestPlus, Alliance of Biodiversity International and the International Center for Tropical Agriculture (CIAT), Cali, Colombia | [6]Department of Information Technologies, Faculty of Economics and Management, Czech University of Life Sciences Prague, Kamýcká, Prague, Czech Republic | [7]Plant Breeding & Genetics Laboratory, International Atomic Energy Agency, Vienna, Austria

Correspondence: Palakolanu Sudhakar Reddy (Sudhakarreddy.palakolanu@icrisat.org)

Received: 14 June 2024 | **Revised:** 20 February 2025 | **Accepted:** 26 March 2025

Funding: P.S. acknowledges the financial support from the Department of Science and Technology, New Delhi, Government of India, for the support from the core grant research (CRG) grant file no. DST No: CRG/2019/004305. The contributions from J.K. are acknowledged and supported by the internal grant agency of the Faculty of Economics and Management, Czech University of Life Sciences Prague, grant no. 2023B0005

Keywords: dhurrin biosynthesis | drought stress | HCN potential | membrane damage | metabolomics | transcriptomics | WGCNA

ABSTRACT

The accumulation of the livestock-harming cyanogenic glucoside dhurrin in the vegetative tissues limits the use of sorghum as a major pasture crop. This study integrates transcriptomics and metabolomics data from the ICSV 93046, CSH 24-MF and ICSR 14001 genotypes, which differ in drought tolerance and cyanide potential (HCNp), to understand the molecular processes of cyanogenesis under drought stress conditions. While ICSV 93046 showed drought adaptation and reduced HCNp, ICSR 14001 and CSH 24-MF exhibited decreased drought stress tolerance with HCN accumulation. The differentially expressed gene (DEG) data showed drought-related genes were significantly upregulated in ICSV 93046 but downregulated in ICSR 14001. KEGG pathway analysis revealed enriched dhurrin biosynthesis and cyanoamino acid metabolism genes, with higher expression in ICSR 14001 than in ICSV 93046. WGCNA analysis revealed that hub genes are involved in drought-induced signalling components, such as phospholipases (PLPs) and lipoxygenases (LOXs), which are implicated in membrane protection. In drought-sensitive genotypes, stress-induced membrane damages lead to the release of dhurrin into the cytoplasm, thus elevating HCN content and activating defence responses. Conversely, the drought-adapted genotype could mitigate HCN production by averting membrane injury, thereby effectively modulating the oxidative stress and preventing the release of dhurrin into the cytoplasm.

Abbreviations: DS, drought stress; FTSW, fraction of transpirable soil water; HCNp, hydrogen cyanide potential; NTR, normal transpiration ratio; TE, transpiration efficiency; WGCNA, weighted gene correlation network analysis; WW, well-watered.

1 | Introduction

Sorghum (*Sorghum bicolor* [L.] Moench) is a versatile crop cultivated as a source of grain, forage and energy (Calviño et al. 2012). The sorghum stover is highly valued as a forage resource due to its high dry matter yield and in vitro digestibility (Terler et al. 2021). Therefore, forage sorghum has significant demand in developed nations (FAOSTAT 2018) as livestock feed (Prasanth et al. 2021). One of the significant constraints in sorghum green forage is a synthesis of prussic acid or hydrogen cyanide (HCN), a toxic defence compound released during herbivore attack or biotic stress from the cyanogenic glucoside compound (dhurrin) (Bak et al. 2006; Morant et al. 2007). Over 2500 plant species synthesize cyanogenic glucoside compounds (Tattersall et al. 2001; Gleadow and Woodrow 2002). Dhurrin, the cyanogenic glucoside compound in sorghum, is a secondary metabolite that acts as a plant defence compound and releases HCN during herbivores, pests and pathogen attacks (Pičmanová et al. 2015). Dhurrin, leading to HCN poisoning, is a significant threat (Cornara et al. 2016; Hayes et al. 2016) for the ruminant livestock that consumes sorghum as forage, leading to symptoms like difficulty in breathing, muscle tremors, staggering, convulsions, collapse and death, which occurs in a short period (Jadav et al. 2019). The fatal poisoning of animals consuming forage sorghum containing high levels of HCN is frequently reported in most countries, including India. Early-stage sorghum plants have higher HCN than the same plant at maturity, indicating that the risk of HCN level decreases as plants mature (> 50 days). Previous studies reported the sub-cellular storage of dhurrin in vacuoles (Saunders and Conn 1978). However, recent studies found the compound in the cytosol (Heraud et al. 2018; Knudsen et al. 2018, 2020; Møller et al. 2021), epidermal protoplasts and mesophyll tissues (Conn 1980). It has been shown that dhurrin is transported to the vacuoles or other compartments (Darbani et al. 2016; Jørgensen et al. 2017).

In sorghum, the dhurrin biosynthetic pathway is well elucidated, and the three primary genes code for the specific enzymes catalysing the formation of dhurrin (Bak et al. 1998; Gleadow et al. 2016; Jones 1998; Kahn et al. 1999; Takos et al. 2011; Katamreddy et al. 2024). Dhurrin biosynthesis pathway, converting L-tyrosine to dhurrin *via* *p*-hydroxymandelonitrile by different enzymes, cytochrome P450s (CYP79A1 and CYP71E1) and UDP-glycosyltransferase (UTG85B1) (Jones 1998; Kahn et al. 1999; Thorsøe et al. 2005; Katamreddy et al. 2024), respectively have been reported. Al-Beiruty et al. (2020) showed that hydrogen cyanide potential (HCNp) levels exceeding 600 ppm have been considered hazardous to the animals. In contrast, the levels below 200 ppm are a threat to the hungry ones. In forage sorghum, HCNp has been estimated at 100–800 ppm on a dry matter basis (Karthika and Kalpana 2017; Jadav et al. 2019). However, other factors influence dhurrin production, leading to HCNp in sorghum, including age, stage of the plant, genotype and environmental conditions (Wheeler et al. 1990). Dhurrin accumulates mainly in the sorghum younger leaves and tillers, further increasing with adverse stresses like drought. Drought restricts plant growth and increases the content of HCNp (Busk and Møller 2002). It is evident from a few studies (Gleadow et al. 2016; Cowan et al. 2020) that drought enhances the accumulation of dhurrin under stress conditions and alters the metabolic pathways involved in the production of specialized compounds like cyanogenic glucosides (Bohnert et al. 1995; Selmar and Kleinwächter 2013). Four-week-old sorghum plants under low soil moisture content can increase the HCNp depending on the severity and duration of stress (Busk and Møller 2002; O'Donnell et al. 2013).

Few studies target the dhurrin biosynthesis pathway genes through breeding, TILLING and gene silencing approaches. These approaches have resulted in a certain degree of success in developing low-HCN sorghum varieties, such as *tcd1* (Blomstedt et al. 2012) and *tcd2* (Blomstedt et al. 2016). Although *tcd1* exhibits low cyanogenic content and maintains normal growth, *tcd2* shows significantly reduced growth due to the mutation in UGT85B1, leading to the accumulation of toxic compounds. This severe growth limitation reduces its viability as a potential fodder crop. This suggests that cyanogenic glucosides may play a vital role in optimal plant growth, likely serving as a nitrogen source during metabolic processes (Pahuja et al. 2014; Karthikeyan and Babu 2015; Pandey et al. 2019). Hence, as various approaches cannot reduce HCN content, understanding the underlying molecular mechanism for cyanogenesis will help us develop low or safer dhurrin content genotypes. In the present study, an attempt has been made to integrate the multi-omics approaches that paved the way for understanding the mechanism of cyanogenesis under drought stress (DS) conditions. Our study identifies the sorghum genotypes contrasting DS tolerance and HCNp accumulation. Transcriptome and metabolomic analysis support our observations with differential expression and abundance of enzymes and compounds related to HCN biosynthetic pathways. Further, the transcription factor (TF) network analysis and weighted gene correlation network analysis (WGCNA) predict the possible TF regulatory networks, hub genes and mechanisms involved in the drought-induced HCN production in sorghum. This study provides valuable information on the regulation of cyanogenesis under DS and probable candidate genes to develop acyanogenic sorghum with improved livestock feed quality and stress tolerance.

2 | Material and Methods

2.1 | Plant Material and Sample Collection

Three genotypes (ICSV 93046, CSH 24-MF and ICSR 14001) of *S. bicolor* were selected for this study. ICSV 93046 is a dual-purpose variety with salinity and terminal drought adaptation with sweet stalks; hence, it is used as a parent in various forage varieties and hybrid development. CSH 24-MF is a forage hybrid released in India and is very popular and occupies an extensive acreage for fodder production because of its fodder quality and yields. ICSR14001 was released as a biofortified sorghum variety 14001 with 45 ppm iron and 32 ppm zinc in grains. All these entries were subjected to progressive DS, HCN potential estimation, transcriptome and metabolome analysis. Leaf tissue samples were collected simultaneously from the plants under DS at 0.25 normalized transpiration rate (NTR) and well-watered (WW) conditions 50 days after sowing (DAS). The samples were immediately snap-frozen in liquid nitrogen for

total RNA extraction and transcriptome analysis. About 1 g of leaf sample was collected in triplicates and used for HCNp and metabolomic analyses.

2.2 | Imposition of Progressive DS and Assessment of Physiological Parameters

The sorghum genotypes, each with 12 replicates, were cultivated in the greenhouse under natural daylight variations, maintaining average day/night temperatures of 28/22°C and relative humidity of 70/90% for 50 days. The experimental setup followed a complete randomized block design (CRBD) to assess plant transpiration response to soil drying in both WW and DS conditions. The 50-day-old vegetative plants were subjected to dry-down experiments to evaluate genotypic transpiration response to soil drying, which is crucial for water-limited environments as described (Kholová et al. 2010; Sivasakthi et al. 2019). Before the experiment, pots were irrigated and allowed to drain to field capacity, with a plastic sheet and beads utilized to minimize water evaporation. Initial pot weights were recorded around 9:00 am, with daily weighing performed to calculate transpiration. Plants were maintained at 80% field capacity for WW conditions, while DS treatment gradually reduced available water, replenishing any losses exceeding 70 g. The experiment concluded when transpiration in all stressed plants dropped below 10% of well-watered plants. Post-experiment, plants were harvested and dried at 60°C for 48–72 h. The fraction of transpirable soil water (FTSW) was determined by calculating the volumetric water content of the soil using the formula: (daily weight – final weight) / (initial weight – daily weight) (Kholová et al. 2010). Subsequently, a segmented regression model was applied to identify potential breakpoints in the relationship between normalized transpiration ratio (NTR) and FTSW, using the 'segmented' function in R. The breakpoints were extracted, and individual plots were generated for each genotype using the ggplot function in R.

Physiological traits, such as total transpiration (TT), transpiration efficiency (TE) and biomass (BM), were measured. The TT is measured as the difference of water lost from each plant from start to end of weighing till the plant reaches 0.1 NTR. TE measures biomass and TT calculated for the WW and DS plants. The stem and leaf of the plants under WW and DS were harvested when the plant reached 0.1 NTR, packed in a bag, and allowed to dry at 60°C for 72 h, and total biomass was calculated.

2.3 | Estimation of HCN Potential

A leaf tissue sample (~1 g) was collected in triplicate from three sorghum genotypes (ICSV 93046, CSH 24-MF, ICSR 14001) at 50 DAS, grown under WW and DS conditions in a glasshouse. The estimation of HCNp in the leaf samples was conducted using the picric acid method described by Hogg and Ahlgren (1942), with modifications from Rezaul Haque and Howard Bradbury (2002) and Pandey et al. (2019). The leaf tissue collected was finely chopped with a scalpel and transferred to a glass tube with 200 μL chloroform. A Whatman No. 1 filter paper strip (1 × 10 cm) pre-soaked in saturated alkaline picric acid was attached to the cork stopper and suspended inside the sealed tube. After 24 h at room temperature, the strip was transferred to a new tube with 5 mL distilled water until the colour was fully released. The hydrocyanic acid released from the plant material reacts with a picric acid solution to form a red isopurpuric acid complex. The intensity of the colour was measured spectrophotometrically at 510 nm, and HCN content was quantified using a standard curve prepared with KCN.

2.4 | RNA Sequencing

The transcriptomics approach dissects the HCN induction mechanism under DS to identify the precise candidate genes. The genotypes varying in the HCN induction under DS were further subjected to RNA sequencing for accurate candidate gene identification. Two biological replicates from three genotypes (ICSV 93046, CSH 24-MF, ICSR 14001) with contrasting drought tolerance and HCN induction were selected for RNA sequencing. Total RNA extraction was carried out in triplicates using 100 mg of the leaf tissues with a Nucleospin RNA Plant kit (Macherey-Nagel, Duren, Germany). According to the manufacturer's instructions, the high-quality total RNA (RIN ≥ 7) was used for transcriptome library construction using the Illumina TruSeq RNA Sample Prep Kit. Libraries were sequenced on the Illumina HiSeq. 2500 platform using the 100 bp paired-end method. The raw sequence reads underwent a quality check using FastQC (Andrews 2010) and Raspberry v0.1 (Katta et al. 2015). Low-quality reads were removed, and sequencing adaptors were trimmed using the software Trimmomatic (Bolger et al. 2014). The resulting trimmed reads were aligned to the *S. bicolor v3.0.1* genome using Hisat2 v2.2.0 (Kim et al. 2015). Finally, feature Count v2.0.2 (Liao et al. 2014) was used to assemble the mapped reads from each sample into transcripts.

2.5 | Transcriptome Analysis

The differential expression analysis was performed using the DESeq.2 package (v1.42.1) in R, with read counts derived from alignment BAM files as input. DS samples (treatment) were compared to the WW samples (control) for each genotype. Transcripts with a log2 fold change greater than or equal to 2 and an adjusted *p*-value of 0.05 or less were considered significantly upregulated. In comparison, transcripts with a log2 fold change less than or equal to −2 and an adjusted *p*-value of 0.05 or less were considerably downregulated. The DEGs were plotted with normalized row counts in heatmaps using TBtools (Chen, Chen, et al. 2020). Gene Ontology enrichment analyses were performed for the DEGs from each genotype using the InterMine interface in the Phytozome13 database (https://phytozome-next.jgi.doe.gov/phytomine/begin.do) and plotted as bubble plots using SRPlot (https://www.bioinformatics.com.cn/en). KEGG (Kyoto Encyclopaedia of Genes and Genomes) pathways of DEGs were obtained from the KEGG Mapper (https://www.genome.jp/kegg/mapper/search.html) and individual KEGG pathways were obtained from the KEGG PATHWAY Database (https://www.genome.jp/kegg/pathway.html). The genotype-wise comparison of DEGs was performed using Venny 2.1 (https://bioinfogp.cnb.csic.es/tools/venny/). The common DEGs obtained from the comparison were used for the

K-means clustering in the MeV expression viewer with 10 clusters and plotted as a heat map with hierarchical clusters using the Euclidean Distance method. The expression curve obtained from MeV and functional annotation (KEGG and GO-biological process) of the clusters was performed using the Plant Geneset Enrichment Analysis toolkit (PlantGSEA) (http://bioinformatics.cau.edu.cn/PlantGSEA/analysis.php).

2.6 | TF Network Analysis

We have performed TF network analysis to identify the TFs and understand their regulatory roles in drought-induced HCN production. Initially, total TFs were filtered out from the total DEGs and classified based on TF families using Plant Transcription Factor Database v5 (http://planttfdb.gao-lab.org/), and a K-means clustering (Euclidean distance method) has been performed based on their normalized expression values using Multi Experiment Viewer v4.9.0 software. The Plant Transcriptional Regulatory Map (http://plantregmap.gao-lab.org/network.php) tool retrieved the regulations among total DEGs, including the TFs. TFs and their targets have been plotted using Cytoscape version 3.9.1 and the ClueGO 2.5.10 plug-in for the functional annotation of the network.

2.7 | Weighted Gene Correlation Network (WGCNA) Analysis for Identifying the Co-Expressing Genes and Module Identification Associated With HCN Induction Pathway Genes

The WGCNA R package established a coexpression network, examining the correlation between modules with physiological and expression data (trait data). The analysis utilized 4538 DEGs obtained from the three separate comparisons with DESeq. 2 normalized expression as an input. The estimation of the soft threshold power was performed using the pickSoftThreshold function. Next, a correlation matrix was generated using the soft threshold power. Subsequently, a topological overlap matrix (TOM) was computed from the transformed correlation matrix. Ultimately, the genes were classified according to their topological overlap dissimilarity (1-TOM) through average hierarchical clustering with the hclust function. Gene modules were subsequently identified using a dynamic tree cutoff algorithm, with a minimum cluster size of 30 and a merging threshold function of 0.25. Module membership (MM) was determined by computing Pearson correlations between the expression level and the module Eigengenes to identify hub genes within the modules. The module Eigengenes has been correlated with each trait data point to establish a relationship between trait data and the network. The gene significance (GS) was employed to establish a correlation between the trait data and the expression data of specific genes.

Cytoscape version 3.9.1 was utilized to visually represent the gene networks in the selected modules and illustrate the biological interactions involving hub genes. To determine the primary genes linked to HCNp within the modules, we initially filtered genes with a GS value greater than 0.2 or less than −0.2 and a MM value greater than 0.7 or less than −0.7, resulting in a set of highly significant genes. Within the sets of these genes, we conducted a more detailed investigation of the genes that showed differential expression. Mercator4 v5.0 (https://www.plabipd.de/mercator_main.html) annotations were used to cluster the significant nodes in the network. GO (biological process) and KEGG functional enrichment analysis of the modules was performed using the Plant Geneset Enrichment Analysis toolkit (PlantGSEA v2.2) (http://bioinformatics.cau.edu.cn/PlantGSEA/analysis.php) (Yi et al. 2013) with Yekutieli (FDR under dependency) with < 0.05 significance level and plotted using the ggplot2 package in R.

2.8 | Metabolomics Extraction and Profiling

The experiment consisted of leaf samples collected from three sorghum genotypes (ICSV 93046, CSH 24-MF and ICSR 14001) with two treatments- well-watered and DS conditions. The samples were collected 50 DAS, flash-frozen in liquid nitrogen, and stored at −80°C for metabolite extraction and analysis. The metabolites were extracted using 60% methanol with 0.1% formic acid (De Vos et al. 2007). Nontargeted metabolomics was conducted to study the HCN-induced metabolites during DS conditions. The metabolites were analysed in a positive ionization mode using a liquid chromatography high-resolution-mass spectrometry (LC-HRMS). LC-MS raw data have been processed with a user-interactive LC-MS data processing tool, MZmine2 (Pluskal et al. 2010).

LC-HRMS-generated raw data were collected, converted into an mzXML file, and imported to a user-interactive mass-spectrometry data processing for analysis and visualization using MZmine2.53. Mass detection, chromatogram building and deconvolution, peak identification and retention time alignment across the samples were performed. Baseline correction was performed before peak detection of all the peaks about the total ion chromatogram. Chromatograms with a peak retention time greater than 0.2 min were built from peaks with $> 10\,000$ intensity. Peaks were deconvoluted using the centWave algorithm, aligned across samples and adducts and isotopic peaks and inconsistent peaks (absent in more than two replicates) were removed. The Data matrix was exported to MS Excel for further statistical analysis. Peaks that were inconsistent among replicates and those annotated as isotopes and adducts were excluded from further analyses. The total compounds were mapped to KEGG Mapper (https://www.genome.jp/kegg/mapper/search.html) for the *S. bicolor*, and mapped compounds with intensity values were filtered out for further analysis. The differential analysis was performed using the DESeq. 2 package, and the significant (padj < 0.05) compounds with high (log2fc > 1) and low (log2fc < -1) abundance have been identified. The crucial compounds were used to perform the pathway enrichment analysis in MBROLE 3 (http://csbg.cnb.csic.es/mbrole3/analysis.php), and the top 10 pathways were plotted using the ggplot2 package in R. The total differential compounds were used for K-means clustering (Euclidean distance method). Enrichment analyses were performed for each cluster using MBROLE 3 and plotted using the ggplot2 package in R.

2.9 | Quantitative Real-Time PCR (qRT-PCR)

About 100 mg of the leaf tissues were collected in triplicates under WW and DS conditions across the selected genotypes. As per manufacturers' guidelines, total RNA was extracted using a nucleospin RNA Plant kit (Macherey-Nagel, Duren, Germany). Following the manufacturer's protocol, it was converted to cDNA using a SuperScript III first-strand cDNA synthesis kit (Invitrogen, Life Technologies, NY, USA). The qRT-PCR was performed in a CFX96 Real-Time System (Bio-Rad, Hercules, CA, USA) with 2X SensiFAST TM SYBR No-ROX (Bioline, UK) as per manufacturer's protocol. The relative expression levels were analysed using the $2^{-\Delta\Delta}$Ct method (Livak and Schmittgen 2001) by normalizing with reference genes *SbElF4α* and *SbPP2A* (Sudhakar Reddy et al. 2016). The primer sequences and gene details used for the qRT-PCR are provided in the Supporting Information S2: Table S4.

2.10 | Statistical Analysis

For progressive DS, the relationship between NTR and a FTSW was analysed with a segmented regression model fitted to the data using the 'segmented' function, which provides a breakpoint value. Two-way ANOVA was conducted to test the genotype and treatment differences for different physiological traits measured under progressive DS and for HCNp estimation using Graph pad Prism version 9.4 (Graph pad software Inc. CA, USA). Means were compared using the Fisher's LSD test with a 95% confidence interval ($p < 0.05$).

3 | Results

3.1 | Identification of Sorghum Genotypes Contrasting for the DS Tolerance

Sorghum genotypes subjected to progressive DS exhibited a clear genotypic difference in declining transpiration (NTR) under decreasing soil moisture content (FTSW) (Figure 1A). During the early vegetative stage exposure to stress, phenotypic differences between the genotypes were detected in the leaf wilting. Higher leaf wilting was observed in the ICSR 14001 and CSH 24-MF genotypes compared to ICSV 93046 (Supporting Information S1: Figure S1A). The genotype ICSV 93046 restricted its transpiration early, reached the FTSW breakpoint at 0.50, and has been considered an efficient drought adaptation strategy compared to other genotypes. The decline in the transpiration rate was first noticed in ICSV 93046 and CSH 24-MF compared with the genotype ICSR 14001. While the genotype ICSR 14001 reached the breakpoint (FTSW) at 0.32 (Figure 1A), genotype CSH 24-MF exhibited a decline in transpiration and reached the breakpoint (FTSW) at 0.38 with medium drought adaptation. Additionally, other physiological traits, including TT and biomass (BM), indicated significant differences among the genotypes under DS compared to those under WW conditions (Supporting Information S1: Figure S1B,C). The water use efficiency (WUE) traits like TE are significantly high ($p < 0.05$) in the tolerant genotypes (Figure 1B), which is intricately connected with photosynthesis.

In this study, various physiological traits were measured, including TE, TT and BM. Significant differences were observed among the treatments and genotypes ($p < 0.05$). Under WW conditions, average TT ranged from 3335.6 to 4277.2 g, BM ranged from 25.4 to 32.4 g (Supporting Information S1: Figure S1B,C), and TE ranged from 7.42 to 7.64 g/kg. Under DS conditions, mean TT ranged from 1609.75 to 2464.8 g, BM ranged from 16 to 19.8 g, and TE ranged from 7.78 to 9.32 g/kg (Figure 1B). The genotypes ICSV 93046, CSH 24-MF and ICSR 14001 exhibited significant variation in traits such as TT and BM under DS conditions. Similarly, genotypes ICSV 93046 and CSH 24-MF were found to be significantly different from ICSR 14001 in terms of TE ($p < 0.001$) (Figure 1B).

3.2 | HCNp Varies Under DS

The HCNp showed variation in the genotypes exposed to DS conditions (Figure 1C). Genotype ICSR 14001 exhibited a significant increase ($p = 0.005$) in HCNp under DS conditions (614.4 ppm) compared to the WW condition (505.2). Whereas genotypes ICSV 93046 displayed a significant reduction ($p = 0.010$) in HCNp under DS conditions (362.9 ppm) compared to WW conditions (459.2 ppm). The CSH 24-MF genotype does not exhibit significant reduction ($p = 0.059$) in HCNp under DS conditions (365.8 ppm) compared to WW conditions (431.3 ppm). Under DS conditions, ICSR 14001 displayed significantly higher levels ($p < 0.001$) of HCNp compared to the other two genotypes (Figure 1C).

3.3 | Transcriptomic Changes During DS and Its Relationship With HCN Induction

RNA sequencing resulted in 35–46 million reads after filtering with a 91%–97% alignment rate to the *S. bicolor* genome. Nearly ~24,000 high-quality reads have been assembled from the RNA-sequencing data and annotated. Mapped transcripts with raw count expression values were used for the downstream analysis. The DEGs obtained under DS conditions include 1885 in ICSV 93046, 2662 in CSH 24-MF, and 2234 in ICSR 14001 (Supporting Information S1: Figure S2). Under stress, the genotypes ICSV 93046, CSH 24-MF and ICSR 14001 showed 802, 1240 and 1199 downregulated and 1083, 1422 and 1035 upregulated genes, respectively.

DEGs have been categorized into three gene ontology (GO) subclasses: biological process (BP), cellular component (CC) and molecular function (MF). Different GO terms were obtained in each subclass with significance ($p < 0.05$), gene count and gene ratio (Supporting Information S1: Figure S3A–C). Stress response-related GO terms were highly enriched in the DEGs of ICSV 93046, including response to oxygen-containing compound (GO:1901700), cell wall biogenesis (GO:0042546), response to water (GO:0009415). In the case of ICSR 14001, the carbohydrate metabolic process (GO:0005975), the response to an endogenous stimulus (GO:0009719), and the response to auxin (GO:0009733) were significantly enriched. These results suggested that stress response pathways are more active in the tolerant genotypes (ICSV 93046). KEGG pathway analysis has been performed to

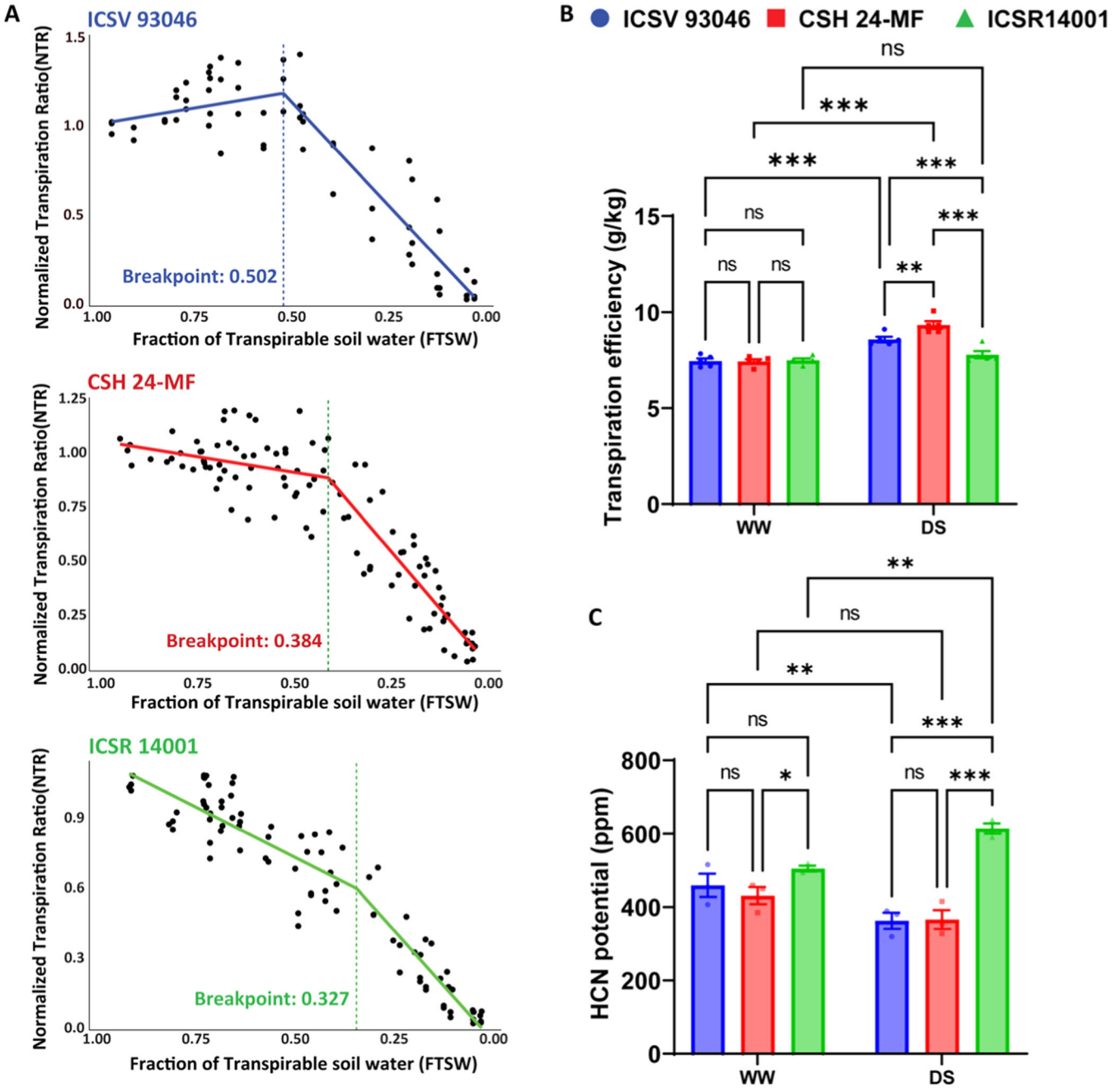

FIGURE 1 | Genotypic variation for transpiration and HCN potential in *Sorghum bicolor* under drought stress. (A) Transpiration difference across the genotypes under progressive drought stress to estimate transpiration losses. The figure shows a fraction of transpirable soil water (FTSW) on the *X*-axis and the Normalized transpiration ratio (NTR) on the *Y*-axis. In ICSV 93046, an FTSW breakpoint at 0.502; in CSH 24-MF, an FTSW breakpoint at 0.384; and in ICSR 14001, an FTSW breakpoint at 0.372 has been observed. (B) Transpiration efficiency (g/kg) and (C) HCN potential (HCNp) estimation were carried by the picric acid method were calculated, and the values obtained are significant as revealed by two-way ANOVA (Fisher's LSD test. ns, $p > 0.05$s, *$p < 0.05$, **$p < 0.005$, ***$p < 0.001$). [Color figure can be viewed at wileyonlinelibrary.com]

understand the metabolic changes due to the DS treatment in each genotype. While 270 KEGG pathways were noticed in ICSV 93046, 329 in CSH 24-MF and 334 in ICSR 14001 were observed. In all three genotypes, a large number of enzymes related to metabolic pathways (ko01100), biosynthesis of secondary metabolites (ko01110), biosynthesis of amino acids (ko01230) and cyanoamino acid metabolism (ko00460) have been found (Figure 2A). In addition, genes related to the MAPK signalling pathway and plant-pathogen interaction were found in all genotypes, suggesting the possibility of activation of defence in response to DS. To understand the HCNp induction mechanism under DS, genotype comparisons were made with the DEGs. A Venn diagram was created to compare the DEGs in all three genotypes. While 462 DEGs were found common in three genotypes, 193 DEGs were common between ICSV 93046 and ICSR 14001 (Supporting Information S1: Figure S3D). A total of 655 DEGs were selected as shared between the contrasting genotypes (ICSV 93046 and ICSR 14001) for drought-induced HCNp, and a K-means clustering analysis was performed using their expression values (log2FC). The K-means clustering analysis resulted in

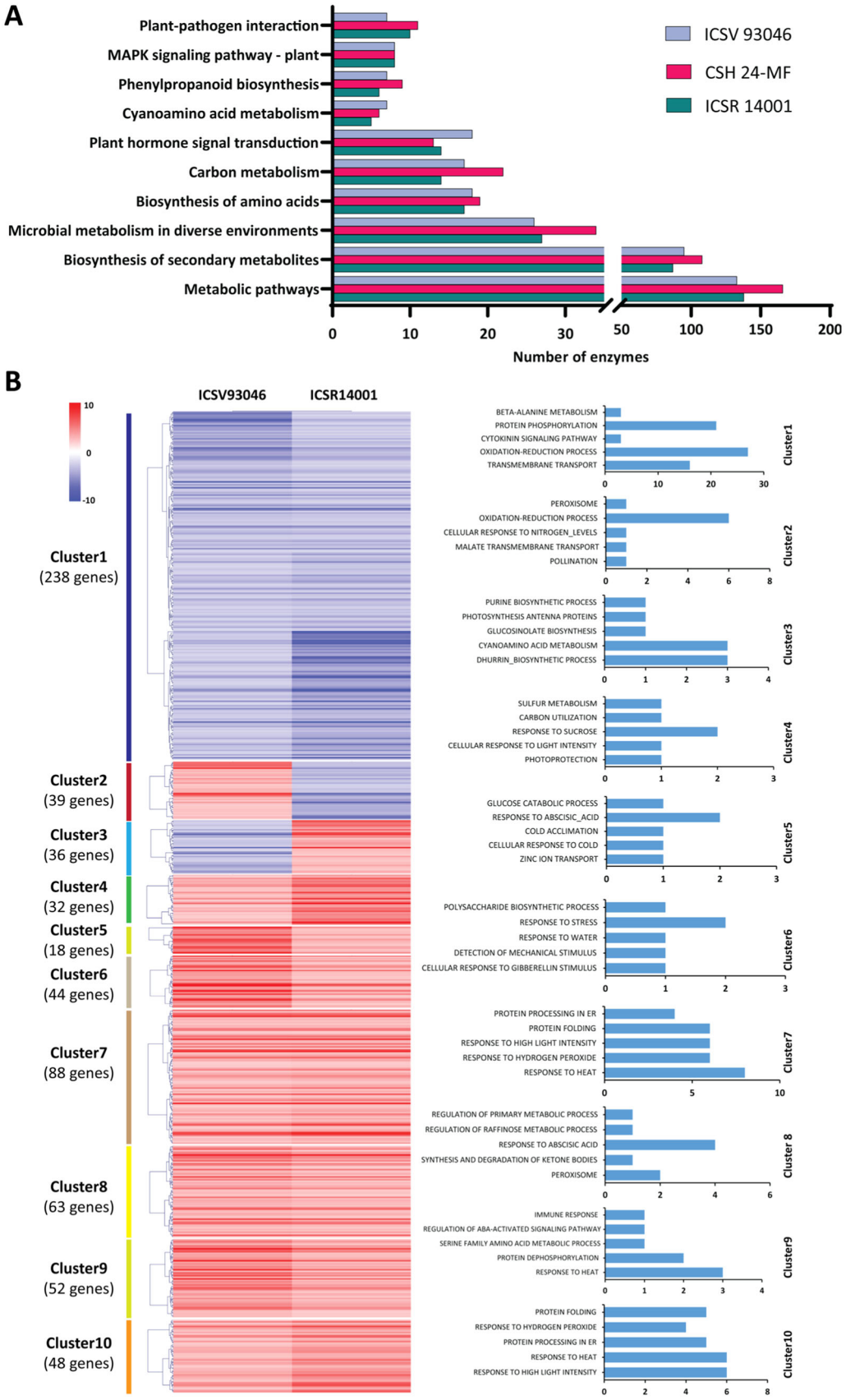

FIGURE 2 | Legend on next page.

10 clusters with differential expression patterns (Figure 2B). Clusters 2 and 3 exhibited a contrasting expression pattern; 39 DEGs were present in cluster 2 with upregulation in ICSV 93046 but downregulation in ICSR 14001. On the other hand, in cluster 3, the gene expressions were downregulated in the ICSV 93046 genotype but upregulated in ICSR 14001 (Figure 2B, Supporting Information S2: Tables S1 and S2). Functional analysis of cluster 2 revealed that stress-related peroxisome, cellular response to nitrogen levels (Figure 2B), and drought-related genes were significantly upregulated in ICSV 93046 but downregulated in ICSR 14001. In cluster 3, the dhurrin biosynthetic pathway, cyanoamino acid metabolism and glucosinolate biosynthesis have been noticed. These contrasting expression patterns infer high HCN levels in ICSR 14001 and low in ICSV 93046 under DS.

3.4 | Transcriptional Regulations During Drought-Induced HCN Production

Three hundred and fourteen TFs from 40 TF families have been identified from all DEGs across three genotypes (Supporting Information S1: Figure S4A). The K-means clustering of these 314 TFs resulted in five differential expression clusters (Figure 3A). Clusters 1, 2 and 3 showed TFs with an average declining expression pattern in all genotypes upon DS. In contrast, cluster 4 showed TFs with mean higher expression were recorded under DS in all three genotypes with 19 ERF and nine bZIP family members. Cluster 5 showed an interesting pattern, in which TFs showed higher expression only in ICSV 93046 under DS with a large number of bZIP (11), MYB (5) and ERF (5) family members (Figure 3A). The TF regulatory network with total DEGs has been created to understand the transcription regulatory patterns involved in drought-mediated HCN induction (Supporting Information S1: Figure S4B). Ten thousand three hundred twenty-three transcriptional regulations among 4538 DEGs have been identified from PlantRegMap with 202 unique TFs and 2835 non-TF genes. Functional analysis (KEGG) of target genes of cluster 4 TFs displayed stress-related pathways such as biotin metabolism, peroxisome, glutathione metabolism, protein processing in ER, and others with cyanoamino acid metabolism as the significant pathway (Figure 3B). Similarly, the target genes of cluster 5 TFs showed glutathione metabolism, sulphur metabolism, porphyrin and chlorophyll metabolism and others with cyanoamino acid metabolism as the significant pathway (Figure 3B). These results surmise the cross-connection between the cyanoamino acid metabolism and drought-induced metabolic pathways in transcriptional regulation (Supporting Information S1: Figure S5A).

Further analysis of the target genes in clusters 4 and 5 using GO (biological process) revealed response to temperature stimulus, abiotic stimulus, response to heat, and cellular water homoeostasis, besides other TFs (Figure 3C). HCN can be produced in plants via cyanoamino acid metabolism and ethylene biosynthesis. Therefore, genes involved in these two pathways were filtered out from all regulations with TFs. TF-network was created to understand the transcriptional regulations of HCN induction under DS with $\log^2$-fold change expression values (Supporting Information S1: Figure S5B). The TF network with reduced expression of ethylene biosynthesis genes suggested that HCN is produced predominantly via the cyanoamino acid metabolism pathway in sorghum genotypes, not by the ethylene biosynthetic pathway. The TF network of HCN-related genes showed that ERF (Sobic.004G295500) are critical for expressing cyanoamino acid metabolism gene UGT85B1 (Sobic.001G012400) and HCN degradation gene thiosulfate thiotransferase (SEN1- Sobic.010G270300) under DS in the ICSR 14001 genotype (Figure 3D). The TF network also disclosed that drought-related TFs, such as MYBs (MYB105, MYB4, MYB98 and MYB105), HSFs (HSFC1, HSFB2A and HSFA6B), bZIPs (ABF1, DPBF1, GBF3 and HY5) and others, might be vital in regulating this pathway under stress (Supporting Information S1: Figure S5B). Additionally, the contrasting expression of TFs such as MYB105, Dof, ERF and HRD between ICSV 93046 and ICSR 14001 genotypes correlated well with the differential expression of their corresponding target enzymes CYP71E1 (Sobic.001G012200) and UGT85B1 (Sobic.001G012400), as well as with the HCN induction pattern (Figure 3D). This suggests a potential role for these TFs in regulating cyanogenesis under DS.

3.5 | WGCNA Analysis to Identify Genes Associated With Drought-Induced HCNp

To explore the genes associated with the drought-induced HCNp, a WGCNA has been carried out using the total DEGs from the transcriptome data set. The trait data, as measured HCNp and TE, have been integrated with an expression of dhurrin biosynthesis genes (Supporting Information S1: Figure S6A,B). We generated 15 expression modules and calculated the correlation between each module and the trait data (HCNp, TE and expression of *CYP71E1, UGT85B1, CYP79A1* and *HNL* genes) (Figure 4A,B and Supporting Information S1: Figure S7A,B). Among these, 'royal blue' was the module most positively correlated with HCNp, containing 140 genes with 114 significant genes (Figure 4B,C). Similarly, 'steel blue' (19 significant genes), 'blue' (126) and 'midnight blue' (15) were the modules that had a higher positive correlation with HCN pathway gene expression (Figure 4B,C, Supporting Information S2: Table S3). The 'pink' (122) and 'dark orange' (36) modules, which were positively correlated with TE but negatively correlated with HCNp, have been considered drought-related modules (Figure 4B,C, Supporting Information S2: Table S3). Most of the module's hub genes unveiled a positive correlation for HCNp and displayed a higher expression in the ICSR 14001

FIGURE 2 | KEGG pathways of all DEGs and cluster analysis of common DEGs between ICSV 93046 and ICSR 14001. (A) The bar graph shows the significant KEGG pathways identified and the genotype-specific DEGs across all three genotypes. The *X*-axis represents the quantity of enzymes present in the pathway, while the *Y*-axis shows the top 10 pathways identified. (B) K-means clustering analysis shows 10 different clusters with expression patterns. Heatmap shows the log2 fold change expression values of common DEGs in the genotypes ICSV 93046 and ICSR 14001. The bar graph shows the corresponding cluster's significant biological process/KEGG pathways, and the *X*-axis represents the number of DEGs present in the corresponding GO term. [Color figure can be viewed at wileyonlinelibrary.com]

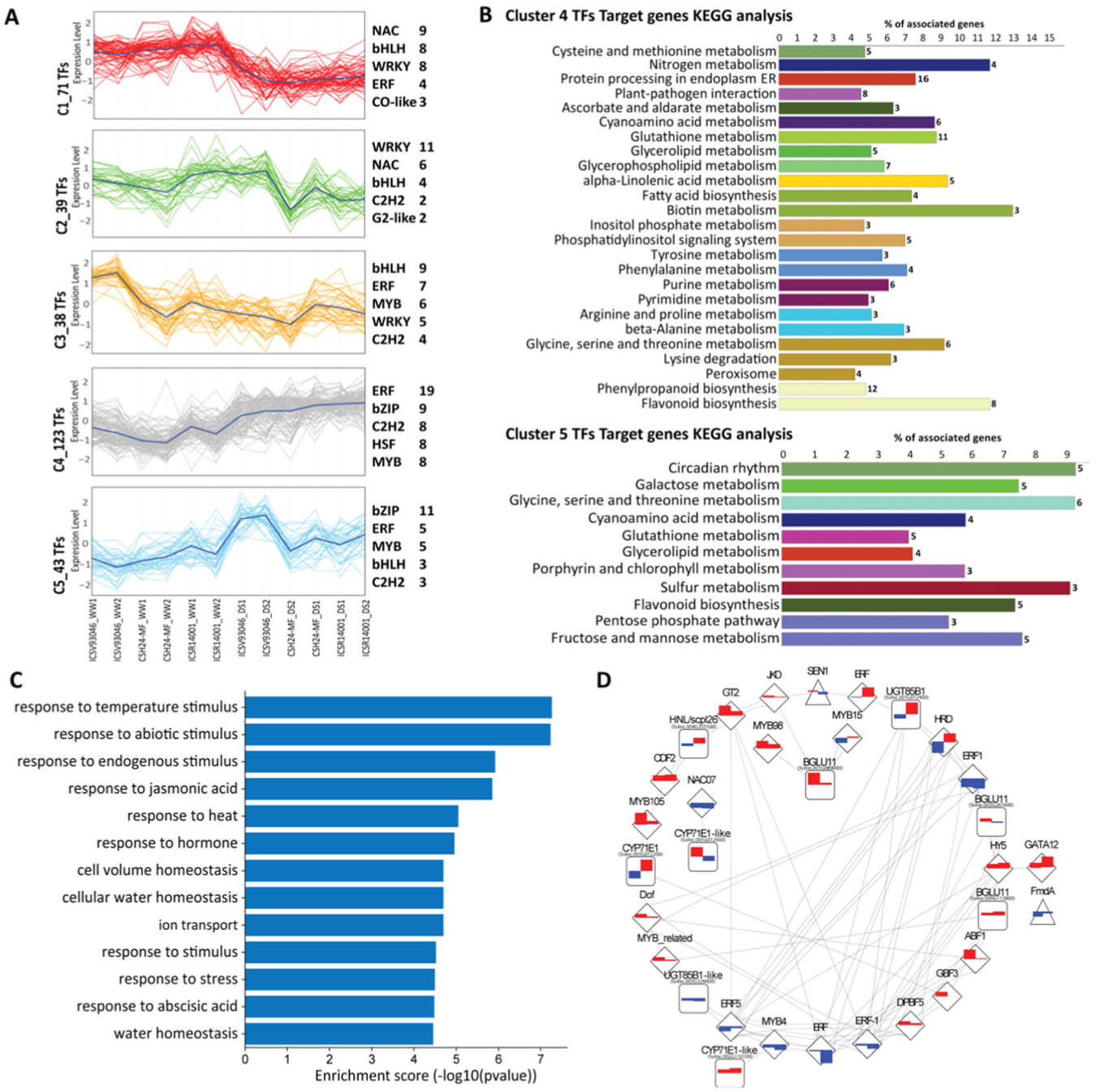

FIGURE 3 | Transcription factor network analysis related to HCN and drought. (A) The figure shows expression curves of the TF clusters obtained by K-means clustering; the middle blue line represents mean expression across samples. Each cluster's top five TF families are shown next to expression curves. (B) Bar graphs represent the significant KEGG pathways (for target genes) identified from the TF network of clusters 4 and 5 TFs. (C) GO biological process enrichment analysis of clusters 4 and 5 TFs' target genes related to drought stress are shown. (D) The TF network of HCN biosynthesis (square with gene ID) and degradation (triangle) genes with their TFs (diamond) are depicted. The bar graph for each gene illustrates the log2FC values in the sequence of ICSV 93046 followed by ICSR 14001. Red bars indicate upregulation, whereas blue bars denote downregulation. [Color figure can be viewed at wileyonlinelibrary.com]

genotype under DS conditions. In contrast, the negatively correlated modules' (pink and dark orange) hub genes exhibited higher expression in the ICSV 93046 genotype but a reduced expression in ICSR 14001 under DS. The hub genes in the royal blue module were SAM-dependent carboxyl methyltransferase (NAMT1), ammonium transporter 1 (AMT1), tropinone reductase 2 (TR-II), RNA recognition motif-containing protein and major facilitator superfamily domain-containing protein (Figure 4D, Supporting Information S2: Table S3). Functional analysis of all significant genes showed purine nucleotide degradation, glycerophosphodiester degradation, methylglyoxal degradation, and others as the significantly enriched pathways (Supporting Information S1: Figure S8). In the steelblue module, three of the top five genes were the biosynthetic enzymes involved in cyanoamino acid metabolism (CYP79A1, scpl26/HNL and CYP71E1), involved in HCN formation from tyrosine.

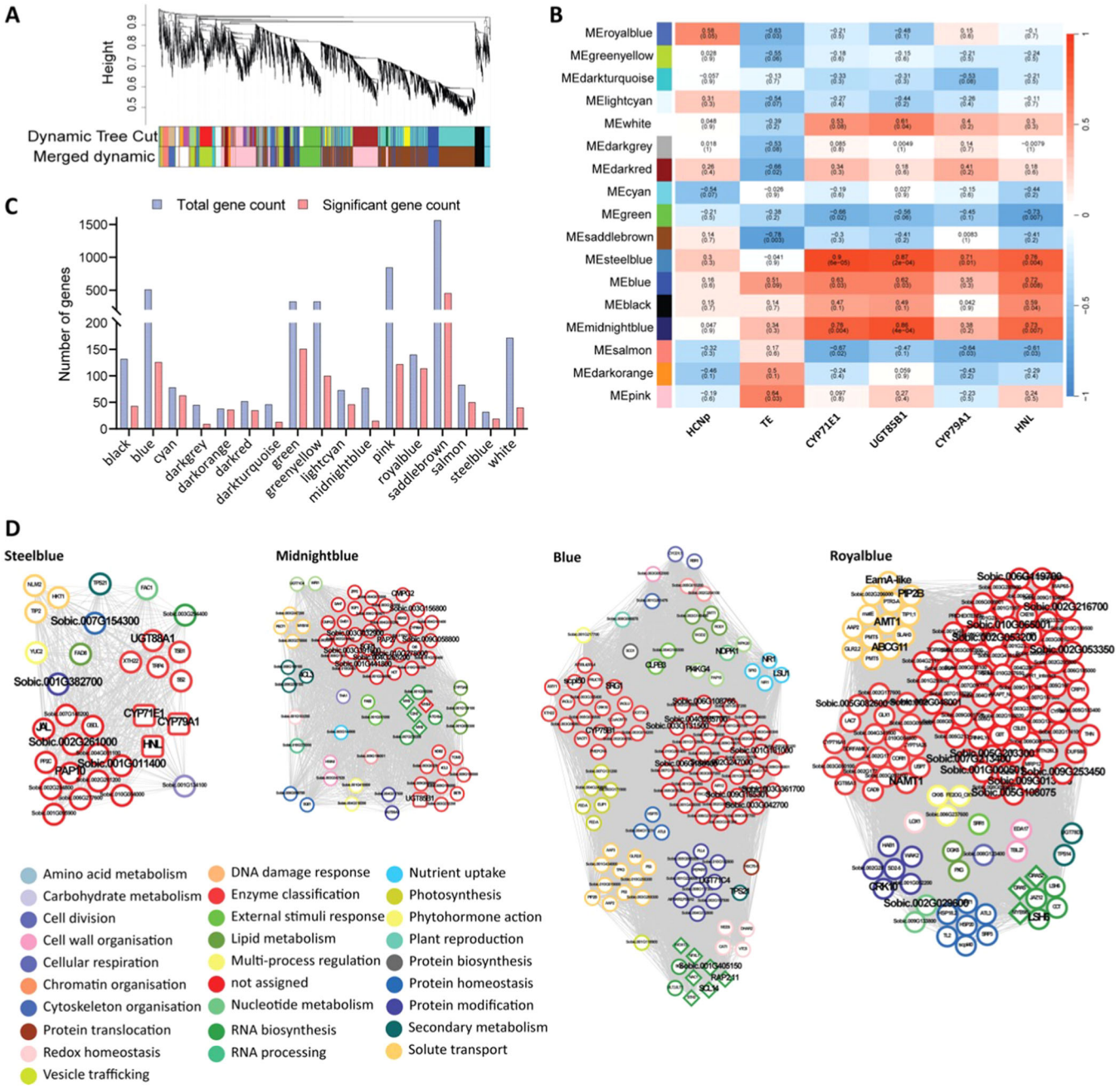

FIGURE 4 | WGCNA analysis to identify genes associated with HCN induction under drought stress. (A) Hierarchical cluster analysis showing the co-expression modules identified by WGCNA. (B) The correlation of the identified modules with the traits and transcription factors. Red and blue reflect positive and negative correlations with gene expression, respectively. The values in each cell represent the corresponding correlation coefficient and *p*-value. (C) The bar graph represents the gene count and significant genes present in each module (gene significance [GS] ≥ 0.2/GS ≤ -0.2). (D) The correlation network represents the significant genes identified for HCNp from different modules. The round square represents the cyanoamino acid metabolism genes, the diamond represents the TFs, and the circle represents all other genes. The node label font size represents the significant gene. Node colour represents the Mercator functional annotation bin names. [Color figure can be viewed at wileyonlinelibrary.com]

Other hub genes in the module included purple acid phosphatase 10 (PAP10), which can catalyse the hydrolysis of inorganic phosphorus (Figure 4D). The enrichment analysis resulted in adenosine nucleotide degradation and cyanoamino acid metabolism as the significant pathways/terms (Supporting Information S1: Figure S8). In the case of midnight blue module dhurrin biosynthetic enzyme UDP-glucosyl transferase 85B1 (UGT85B1-Sobic.001G012400), alpha/beta-hydrolases superfamily protein, U-box domain-containing protein, C2H2 zinc finger protein, and a protein of unknown function DUF688 were the top five hub genes obtained (Figure 4D). The functional analysis displayed phenylpropanoid biosynthesis, 4-hydroxybenzoate biosynthesis and flavonoid biosynthesis, among others, as the significant pathways in the midnight module (Supporting Information S1: Figure S8). The module blue contains UDP-glucosyl transferase 71C4 (UGT71C4),

phosphoinositide 4-kinase gamma 4 (PI4K G4), SCARECROW-like 14 (GRAS2/SCL14) and two uncharacterized proteins (Sobic.009G185301 and Sobic.001G181000) as the top hub genes (Figure 4D). The enrichment analysis of the significant genes displayed the ascorbate glutathione cycle, starch degradation, and L-ascorbate degradation as the major pathways (Supporting Information S1: Figure S8). Together, these results propound that DS leads to nucleotide degradation, secondary metabolism and HCN pathway activation in the ICSR 14001 genotype. These factors appear to contribute to higher HCNp accumulation in this genotype than in other genotypes. In the pink module (negatively correlated for HCNp), beta-1,3-N-acetylglucosaminyltransferase family protein, copper transport protein family, 1-aminocyclopropane-1-carboxylate oxidase protein (ACO4), MYB domain protein 105 (MYB105) and pectin lyase-like superfamily protein were the hub genes identified (Figure 5A). Functional analysis displayed ajugose biosynthesis, linoleic acid metabolism, lysine degradation and other significant pathways (Supporting Information S1: Figure S8). In the hub genes of the dark orange module, folic acid binding protein, peroxidase, beta-glucosidase 13 (BGLU13), phospholipase A 2 A (PLP2) and PATATIN-like protein 4 (PLP4) have been noticed (Figure 5A). Enrichment analysis mainly showed the pathways of phospholipases, asparagine biosynthesis and triacylglycerol degradation (Supporting Information S1: Figure S8). The stress-response pathways, the associated genes, and TFs in ICSV 93046 might generate DS-tolerant genotypes in *S. bicolor*.

3.6 | Validation of Transcriptomics and WGCNA Data

Expression analysis was performed to validate the transcriptome and WGCNA analysis results. The genes selected for validating the data include the dhurrin biosynthesis pathway (*CYP79A1*, *CYP71E1* and *UGT85B1*) and cyanoamino acid metabolism consisting of glycosyl hydrolases (*Sobic.001G089000, Sobic.008G080600* and *Sobic.009G113800*), *hydroxynitrile lyase (Sobic.004G335500)* and *formamidase (Sobic.003G306700)*. In addition, hub-genes from the pink and dark orange modules including *LOX5 (Sobic.006G248300)*, *PER1 (Sobic.002G391100)*, *LOX1 (Sobic.003G385500)*, *CHIA (Sobic.002G055700)* and TFs from the TF-network analysis such as ERF (Sobic.004G295500) and MYB (Sobic.010G106601) were analysed. Moreover, stress-related pathways enriched from transcriptome data and the genes belonging to different KEGG pathways, including phenylpropanoid biosynthesis, MAPK signalling pathway, biosynthesis of amino acids and plant hormone signalling, have been validated. The genes from these pathways were selected for qRT-PCR validation including universal stress protein family (USP), mitogen-activated kinase (MAPK), jasmonate zim domain-containing protein (JAZ), serine/threonine-protein kinase (Sr/Th-Kin), dehydrin (DHY), calcium-binding domain-containing protein (EF-Ca2), late embryogenesis abundant (LEA), small heat shock proteins (sHSP20), nitrite reductase (FeNR), ABA hydroxylase, heavy metal transport (HM detox) and abscisic acid receptor (PYL4). The cyanoamino acid metabolic pathway and other genes described above followed a similar gene expression pattern to the RNA-sequencing data (Figure 5B, Supporting Information S1: Figure S9).

3.7 | HCN Induction-Related Metabolomic Alterations Under DS

An untargeted metabolomics analysis was performed to understand the drought-induced HCN induction at the metabolomic level. KEGG database mapping for *S. bicolor* resulted in 441 metabolites. The differential analysis resulted in 110 (ICSV 93046), 171 (CSH 24-MF) and 148 (ICSR 14001) compounds in the contrasting genotypes under DS. The compounds were plotted as a volcano plot with log2 fold change and their significance [$-\log10(p)$] (Supporting Information S1: Figure S10A) and as a heatmap with log2 normalized abundance value (Supporting Information S1: Figure S10B). Analysis of the significant metabolites included the purine metabolism (sbi00230), biosynthesis of cofactors (sbi01240), cyanoamino acid metabolism (sbi00460), ABC transporters (sbi02010), arginine and proline metabolism (sbi00330), biosynthesis of amino acids (sbi01230), valine, leucine and isoleucine biosynthesis (sbi00290), arachidonic acid metabolism (sbi00590), cysteine and methionine metabolism (sbi00270) and glucosinolate biosynthesis (sbi00966) as the highly enriched pathways across three genotypes (Supporting Information S1: Figure S10C). Further, to understand the contrasting metabolites across these genotypes and conditions, all differentially abundant compounds have been grouped into five clusters (Figure 6A). Cluster 1 contains compounds with a high mean abundance in ICSV 93046 and CSH 24-MF genotypes and a low abundance in ICSR 14001, irrespective of experimental conditions. Cluster 2 showed metabolites exhibiting high abundance in ICSR 14001 in control and DS conditions and ICSV 93046 only under DS conditions. Metabolites in cluster 3 exhibited a high abundance in CSH 24-MF and ICSR 14001 genotypes, irrespective of the conditions. Cluster 4 metabolites exhibited a high abundance in all three genotypes under DS. Cluster 5 compounds showed high abundance in control conditions in all genotypes, whereas, after DS, these compounds displayed a low abundance in CSH 24-MF and ICSR 14001. Still, in the tolerant genotype (ICSV 93046), they showed higher abundance (Figure 6A). This suggests that some compounds in Clusters 4 and 5 might be involved in DS tolerance of the genotype ICSV 93046. Further, the enrichment analysis of these metabolites from each cluster revealed DS-related and defence-related KEGG pathways. Arachidonic acid (AA) metabolism, alpha-linolenic acid (ALA) metabolism, lysine degradation, plant hormone signal transduction, nicotinate and nicotinamide metabolism, taurine and hypotaurine metabolism, along with valine, leucine and isoleucine biosynthesis were the key terms enriched in relation to DS and defence (Figure 6B). In addition, the cyanoamino acid metabolism pathway was one of the pre-eminent pathways in clusters 2, 4 and 5 (Figure 6B). The compounds found in the cyanoamino acid metabolism have been pulled out and shown as a heatmap (Figure 6C), which suggests that under DS conditions, the intermediate metabolites of HCN are copious in ICSV 93046 and ICSR 14001. In contrast, in CSH 24-MF, most of the compounds were unchanged.

Based on the metabolomic and transcriptomic data, cyanoamino acid metabolism was further analysed by mapping the DEGs and differentially abundant metabolites in this pathway (Figure 7). In the case of the ICSV 93046 genotype, most of the enzymes involved in dhurrin metabolism showed downregulation compared to the

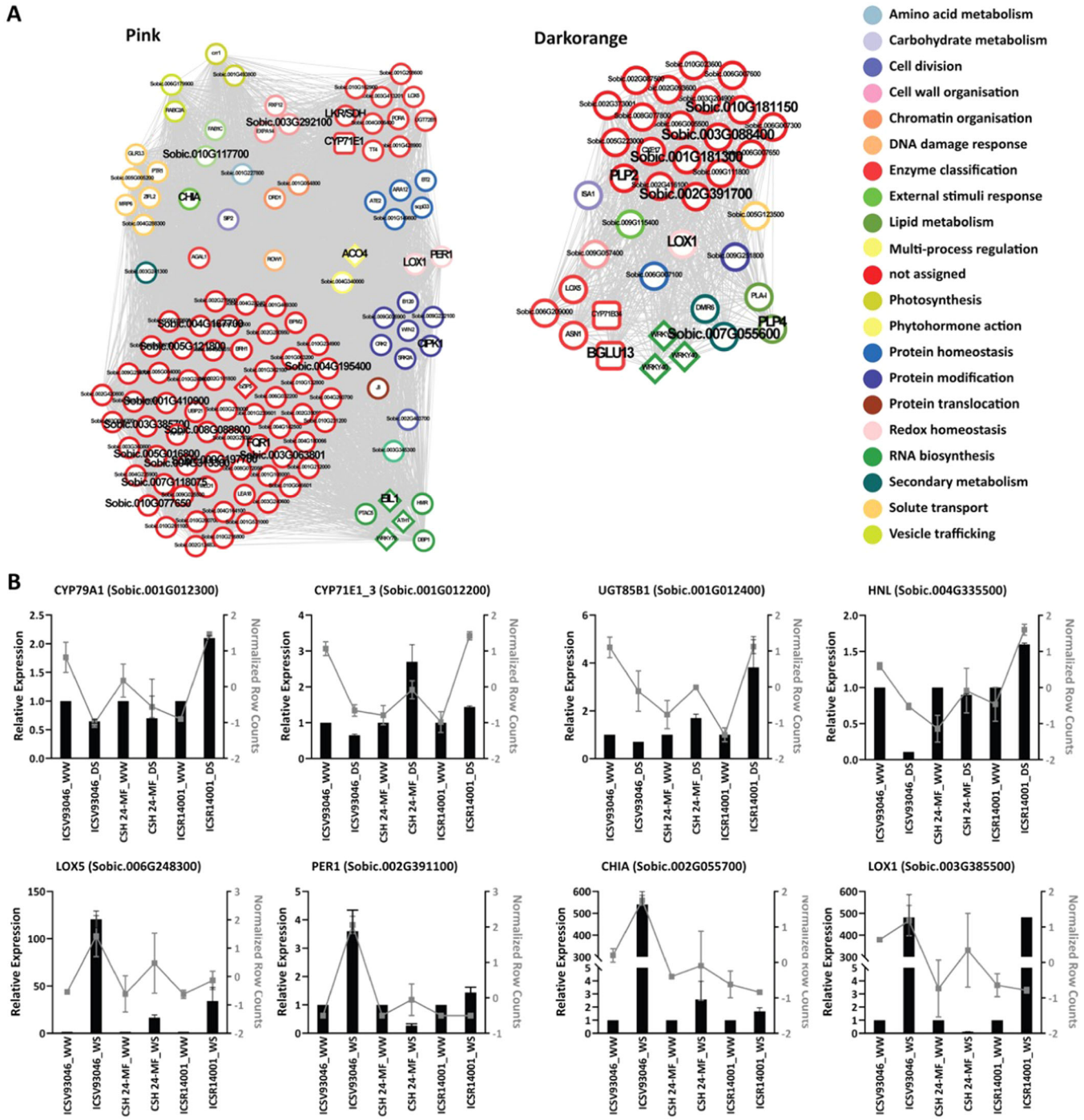

FIGURE 5 | WGCNA analysis to identify genes associated with drought stress. (A) The correlation network represents the significant genes identified for TE from different modules. The round square represents the cyanoamino acid metabolism genes, the diamond represents the TFs, and the circle represents all other genes. The node label font size represents the significant gene. Node colour represents the Mercator functional group. (B) Bar-line graphs represent the qRT-PCR relative expression (black bars) and RNA-seq normalized expression (grey line) of HCN biosynthetic pathway genes across genotypes and conditions. CHIA, acidic endochitinase; CYP71E1, 4-hydroxyphenylacetaldehyde oxime monooxygenase; CYP79A1, tyrosine N-monooxygenase; HNL, Hydroxynitrile lyase; LOX1, lipoxygenase 1; LOX5, 5-lipoxygenase; PER1, 1-Cys peroxiredoxin; UTG85B1, UDP-glycosyltransferase. [Color figure can be viewed at wileyonlinelibrary.com]

WW condition. In contrast, in ICSR 14001, these enzymes displayed upregulation (Sobic.001G012300, Sobic.001G012200 and Sobic.001G012400). Moreover, enzymes (hydroxymandelonitrile lyase [EC:4.1.2.11]) that can convert (S)-4-hydroxymandelonitrile into HCN were significantly upregulated in ICSR 14001 and CSH 24-MF. In contrast, in ICSV 93046, these enzymes have been shown downregulated (Sobic.005G186500 and Sobic.004G335500). Similarly, in the case of metabolites, tyrosine and dhurrin showed significantly high abundance in CSH 24-MF and ICSR 14001, but (E)-4-hydroxyphenyl acetaldehyde oxime, L-valine, 3-cyano-L-alanine and (E)-phenylacetaldoxime exhibited high abundance in ICSV 93046 and ICSR 14001 (Figures 6C and 7). The level of

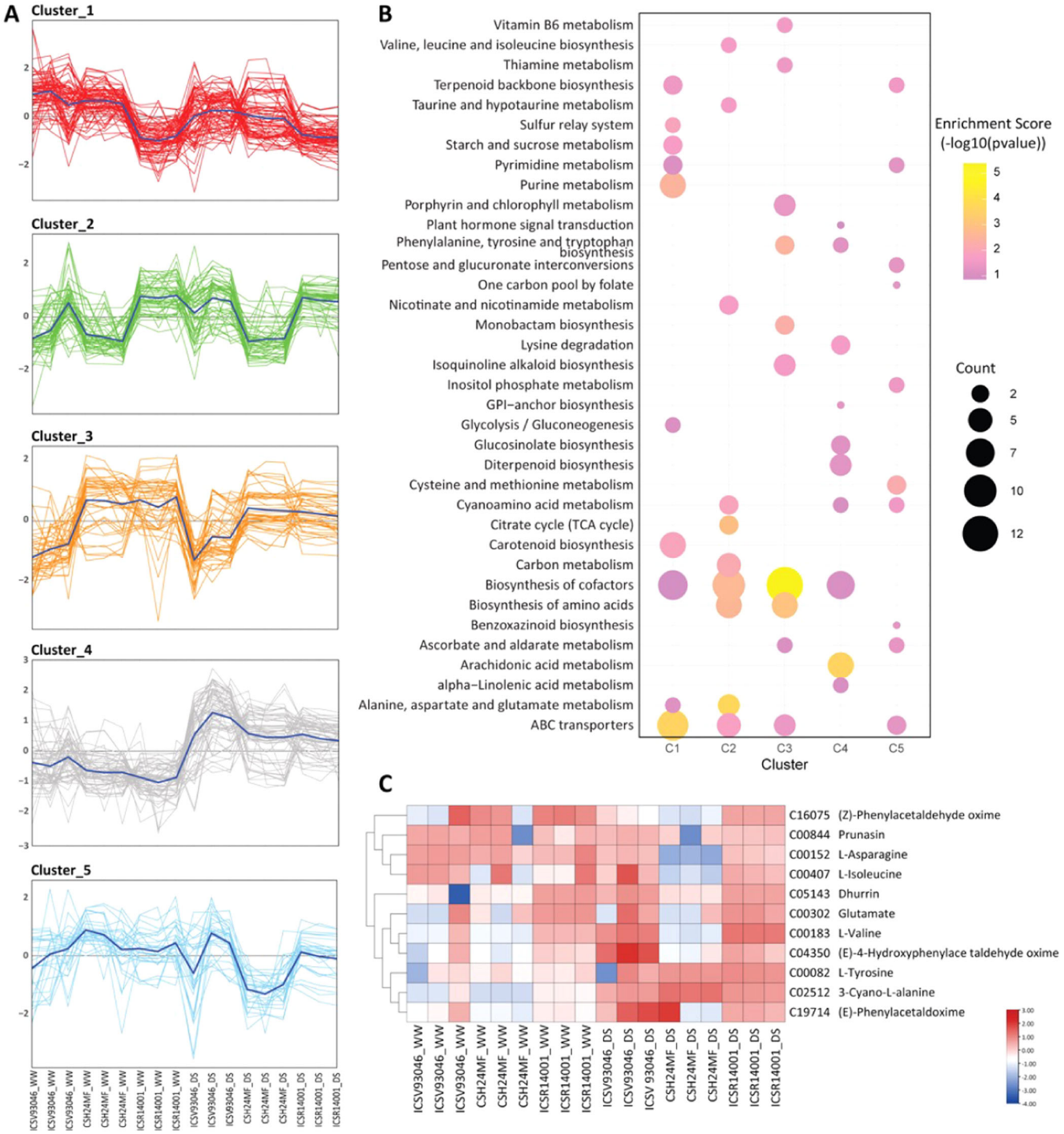

FIGURE 6 | Metabolomic changes under drought stress. (A) Metabolite abundance curves showing the K-means clusters obtained from the 243 compounds resulted in differential analysis of all three genotypes. (B) Enrichment plot showing the top KEGG pathways enriched in corresponding clusters, enrichment ratio calculated as –log10 (*p*-value) and represented as colour scale violet to yellow, and the bubble size represents the number of compounds identified in the corresponding pathway. (C) Heatmap showing the normalized abundance of the metabolites identified from the Cyanoamino acid metabolism pathway. The colour scale represents metabolites' high (red) and low (blue) abundance. [Color figure can be viewed at wileyonlinelibrary.com]

dhurrin in ICSR 14001 was lower than in ICSV 93046, suggesting it may be converted to HCN by the HNL enzyme in ICSR 14001, as indicated by the high HCNp observed experimentally. Like the detoxified product of HCN, 3-cyano-L-alanine was also found to be less in ICSR 14001 than in other genotypes, suggesting its slower degradation. Drought-induced expression changes of these enzymes and the accumulated metabolites support the contrasting drought-induced HCNp in these genotypes and indicate that DS can increase the HCN content in the ICSR 14001 genotype. Contrarily, in other genotypes, stress-responsive mechanisms might prevent the accumulation of HCN or promote its detoxification to confer stress tolerance. Moreover, metabolites associated with the

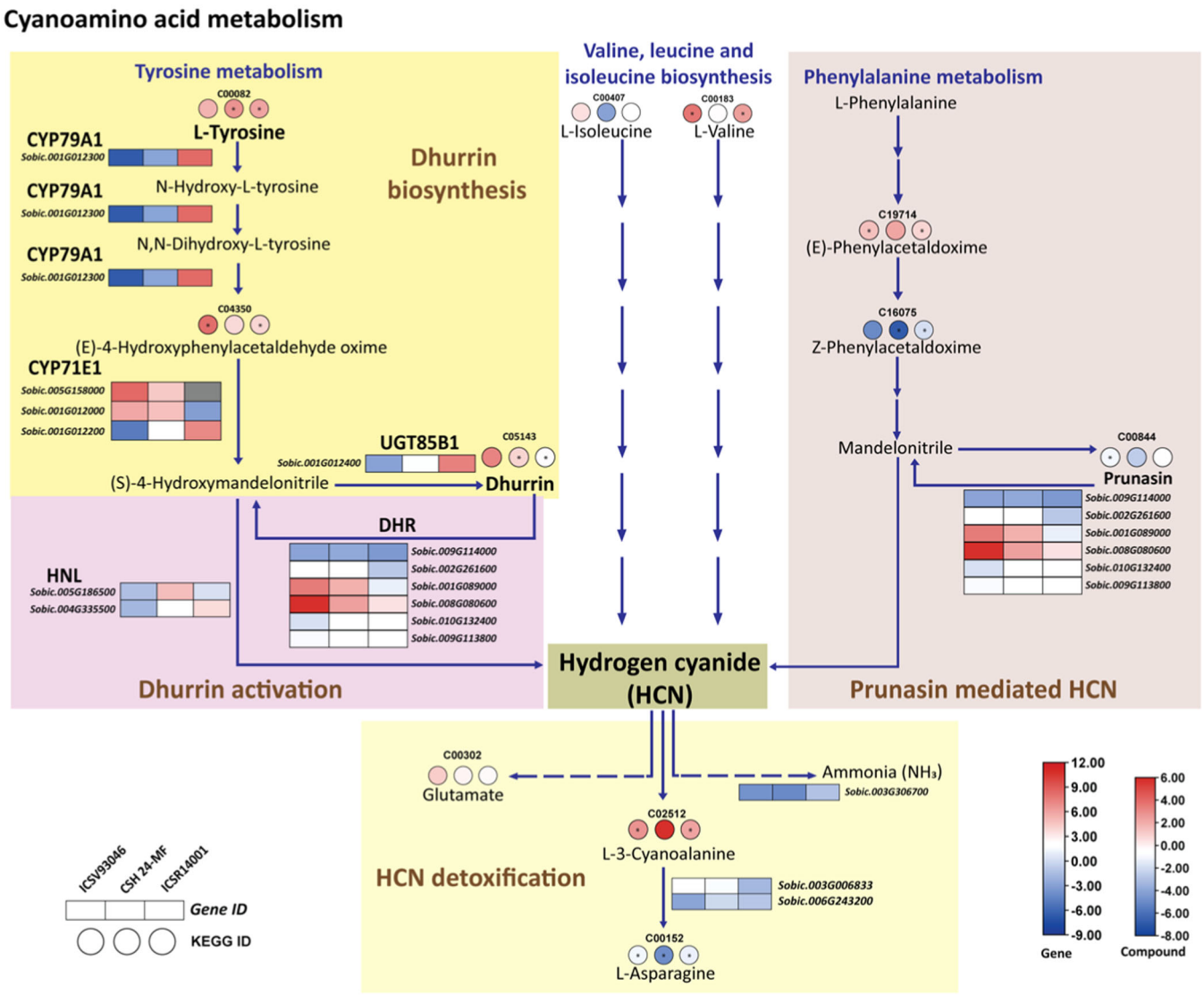

FIGURE 7 | Differential regulation of the Cyanoamino acid metabolism pathway under drought stress. Cyanoamino acid metabolism pathway showing the expression (log2 fold change) of enzymes and compounds identified in the pathway. Squares represent the enzymes/transcript, and rounds represent the compounds. The colour scale represents the log2 fold change expression. Red represents upregulation, and blue represents downregulation. Asterisks in the compounds represent the significance of abundance ($p < 0.05$). The bottom left square boxes represent the gene expression data (log2 fold change), while the circles indicate the compound abundance according to the genotypes—ICSV 93046, CSH24-MF and ICSR 14001. [Color figure can be viewed at wileyonlinelibrary.com]

phenylalanine-derived cyanogenic glucoside prunasin have been identified, including the intermediate compounds (E)-phenylacetyl oxime and (Z)-phenylacetyl oxime, as well as prunasin itself (Figure 7). This suggests that prunasin-mediated HCN biosynthesis may occur in *S. bicolor*.

4 | Discussion

The cyanogenic glucoside, dhurrin found in various tissues of sorghum species (Kahn et al. 1997), is a precursor to HCN. Earlier reports show that the cyanogenic glucoside compound present in sorghum increases DS conditions (Bohnert et al. 1995; O'Donnell et al. 2013; Selmar and Kleinwächter 2013; Gleadow and Møller 2014; Neilson et al. 2015; Gleadow et al. 2016). In addition, there have been reports of negligible amounts of dhurrin in wild sorghum species correlating with differential expression of dhurrin synthesis genes compared to domesticated species under drought-stressed conditions (Ananda et al. 2022). However, the relation between DS and HCN induction in sorghum remains unresolved. Our study aimed to demonstrate the molecular mechanism behind dhurrin biosynthesis and cyanogenesis in contrasting sorghum genotypes under DS conditions by integrating physiological, biochemical, transcriptomic and metabolomics approaches.

4.1 | Relationship Between Drought and HCN Production in *S. bicolor* Genotypes

Transpiration response to soil drying is considered a necessary trait to confer drought adaptation in sorghum (Shekoofa and Sinclair 2018; Sinclair et al. 2005; Vadez et al. 2024). Previous studies have demonstrated genetic variability in sorghum

regarding the FTSW threshold, indicating the initiation of reduced transpiration and biomass accumulation (Gholipoor et al. 2013; Karthika et al. 2019; Choudhary et al. 2019; Djanaguiraman et al. 2024). The observed variations in breakpoints (FTSW) underscore distinct levels of drought tolerance among sorghum genotypes (Figure 1A). The reports show that exposure to DS increases the production of HCN in sorghum (Duncan 1996; O'Donnell et al. 2013; Pandey et al. 2019). Our study shows that the drought-induced HCN production was high in the ICSR 14001 genotype, which has a low breakpoint value. The high breakpoint (ICSV 93046) genotype reduced HCN production (Figure 1C), suggesting that drought sensitivity leads to high HCN production, and drought tolerance mechanisms might reduce HCN accumulation under drought conditions. Native (wild) sorghum species are more tolerant to drought (Cowan et al. 2020) and contain low dhurrin content in the leaves, with cyanogenesis differentially modulated under drought (Ananda et al. 2022). These studies thus point out that wild species are the potential candidates for generating *S. bicolor* lines with negligible dhurrin content in the leaves with high drought tolerance.

4.2 | Regulation of Cyanogenesis Under DS

In sorghum, tyrosine-derived dhurrin has been reported to be the most abundant cyanogenic glucoside (Bak et al. 2006; Møller 2010; Gleadow and Møller 2014). The three significant enzymes (CYP79A1, CYP71E1 and UGT85B1) in the dhurrin biosynthesis pathway, dhurrinase (DHR) and α-hydroxynitrilase (HNL) as critical enzymes appear responsible for the bio-activation of dhurrin to produce HCN. The clustering and KEGG pathway analysis indicated that cyanoamino acid metabolism, dhurrin biosynthesis and glucosinolate biosynthesis are the pathways with high gene expression in the drought-sensitive genotypes compared to the tolerant ones (Figure 2A,B). The HCN estimation revealed significant accumulation potential in the contrasting genotypes under DS (Figure 1B). The cyanoamino acid pathway transcripts and metabolites showed a similar differential expression pattern between the drought-stress genotypes (Figure 7). In addition, the WGCNA analysis unlocked that *CYP79A1*, *CYP71E1* and *HNL*, the hub genes in the steel-blue module, positively correlated with the HCNp (Figure 4D). Similarly, *UGT85B1* has been found as a hub-gene in the midnight blue module, and another module positively correlated with HCNp (Figure 4D). Moreover, the metabolomic analysis demonstrated a higher abundance of cyanoamino acid metabolism intermediates in the sensitive genotypes (Figure 6C). Taken together, these results showed that drought-sensitive genotypes have high HCN production under DS by upregulating the expression of cyanoamino acid metabolism genes, such as *CYP79A1*, *CYP71E1*, *UGT85B1*, *DHR* and *HNL*. At the same time, the genotype showing drought tolerance displayed a contrasting expression pattern, suggesting that DS tolerance prevents the accumulation of HCN under DS conditions by modulating these gene expressions. In other words, drought sensitivity can lead to the accumulation of HCN. The reduced HCN potential in drought-tolerant sorghum genotypes is primarily attributed to the downregulation of key genes involved in HCN biosynthesis and metabolism (Zhang et al. 2023). Sorghum's antisense-mediated downregulation of the *CYP79A1* gene has shown promise in reducing HCN levels (Pandey et al. 2019). Additionally, drought-tolerant varieties may possess enhanced mechanisms for HCN detoxification and utilization, further contributing to their lower HCN potential under stress conditions. Plants have evolved to detoxify HCN and potentially use it as a nitrogen source (Krasuska et al. 2023), demonstrating the adaptability of plant metabolism to environmental challenges and nutrient availability. DS significantly affects nitrogen utilization, thereby affecting plant growth, biomass and yield (Hoang et al. 2018). However, the extent of this effect varies among different sorghum genotypes, with drought-tolerant lines exhibiting higher nitrogen efficiency under water stress conditions (Fan and Li 2001).

4.3 | Transcriptional Regulators of Drought-Induced HCN Induction

Ethylene response factor (ERF) family TFs in plants form a complex network that regulates different abiotic and biotic stresses with varying dynamic patterns and have a mutual influence on each other's function (Van den Broeck et al. 2017; Sharmin et al. 2020; Liu et al. 2021; Yu et al. 2022). The present study demonstrates that some ERF, Dof and MYB members have similar or contrasting expression patterns to their target genes, such as cyanoamino acid metabolic pathway genes *UGT85B1, CYP71E1* and *HNL*. The expression levels of HRD (Sobic.006G184700) and ERF (Sobic.004G295500) were comparable to those of their target gene UGT85B1 (Sobic.001G012400), suggesting that these ERFs may act as positive regulators or transcriptional activators of UGT85B1 under DS. Conversely, MYB105 (Sobic.007G137101) and Dof (Sobic.006G267900) displayed contrasting expression patterns in relation to their target gene CYP71E1 (Sobic.001G012200), indicating that these may function as transcriptional repressors of CYP71E1 under DS. The TF-target interaction requires functional validation for further conclusions. Previous studies also indicate that ERFs are involved in biotic stress tolerance, such as defence against pathogens and herbivores, by activating defence response pathways (Lu et al. 2011; Meng and Zhang 2013; Takafuji et al. 2020; Wu et al. 2020). Taken together, upregulation of ERFs and their target genes of cyanoamino acid metabolism in the sensitive genotype (ICSR 14001) suggests that under drought conditions, induced signalling response might lead to activation of plant defence mechanisms such as bio-activation of cyanogenic glucoside dhurrin, leading to high HCN accumulation. In addition, TFs like *MYB105*, *MYB4* and *Dof* showed higher expression in drought-tolerant genotypes compared to sensitive genotypes (Figure 3D, Supporting Information S1: Figure S5B). We speculate that the HCN production under DS in tolerant genotype is prevented by upregulation of TFs to suppress cyanoamino acid metabolism genes by acting as transcriptional repressors/enhancers of dhurrin biosynthesis genes. MYB TFs play crucial roles in plant responses to DS (Seo et al. 2011; Abhilasha and Roy Choudhury 2021; Qu et al. 2022). Interestingly, some MYB proteins can act as repressors in plant defence responses (Wei et al. 2017). Previous studies have reported the role of Dof family TFs in drought tolerance and secondary cell wall biosynthesis (McCarthy et al. 2010; Dubos et al. 2010; Katiyar et al. 2012; Corrales et al. 2014; Chen, Yan, et al. 2020; Choi

et al. 2023), suggesting the possible role of these TFs in regulation of cyanogenesis under DS, whereas their direct role in the modulation of cyanogenesis needs functional validation.

4.4 | Drought-Stress-Induced Membrane Damages Lead to HCN Induction in Sensitive Genotypes

Abiotic stresses like drought and heat can severely affect the cell membrane, leading to extensive damage to the plant (ElBasyoni et al. 2017; Zayed et al. 2023) due to disturbance of the cell membrane, resulting in loss of membrane integrity by modifying the physical properties of lipids (Osakabe et al. 2013). In plant cells, cyanogenic glucosides are stored in membrane-bound vacuoles, and the bio-activation enzymes are found in the cytosol. Damage to the vacuolar membrane by herbivores via chewing or due to drying allows the contact between glycosides and enzymes, which leads to bio-activation and production of HCN. Environmental stressors, including high nitrogen fertilization under full light and exposure to heavy metals like cadmium, can significantly elevate HCN potential in plants. Nitrogen fertilization boosts HCNp, while cadmium exposure triggers root exudate release and increases thiolic groups within the plant, collectively enhancing conditions for HCN production (Wheeler et al. 1990; Pinto et al. 2006). In addition, osmotic stress can directly induce the production of dhurrin and triglochinin in *Eschscholtzia californica* (Hosel et al. 1985). The results indicate that the environmental stresses can cause membrane damage and induce HCN production. In the present study, KEGG pathway analysis of cluster 4 and 5 TF-targets and the metabolomic analysis revealed enrichment of lipid metabolic pathways (Figure 3B). In addition, enrichment analysis of WGCNA modules showed that in drought-related modules (dark orange and pink), lipid metabolism, triacylglycerol metabolism, phospholipases, linoleic acid metabolism, oxylipin biosynthetic process are the key pathways (Supporting Information S1: Figure S8), suggesting the membrane readjustments to cope up with the stress in tolerant genotype. Previously, plant defence-related pathways have been found altered in the transcriptomic analysis of sorghum seedlings experiencing osmotic stress (Dugas et al. 2011), implying the possibilities of abiotic stress induced damages activate plant-defence response. The nicotinate and nicotinamide metabolism, valine, leucine and isoleucine biosynthesis pathways enriched in cluster 2 of metabolomic analysis (Figure 6B) suggest the possible induction of defence signalling under DS in sensitive genotype. Nicotinate and nicotinamide metabolism are crucial for maintaining redox balance and energy transfer through NAD^+ and $NADP^+$, which act as defence-signalling molecules during pathogen attacks (Gakière et al. 2018). Additionally, valine, leucine and isoleucine amino acids provide flexibility in carbon and nitrogen allocation, especially under drought, and serve as precursors to defensive compounds like glucosinolates, which aid in pathogen resistance (Binder 2010; Kitainda and Jez 2021). These observations infer that drought-tolerant plants rely on active protection and membrane repair mechanisms to mitigate cellular damage, while drought-sensitive plants, in contrast, activate defence responses through increased HCN production in response to drought-induced osmotic stress and damage. Moreover, the hub genes from the drought-related modules included membrane and cell wall modifying genes such as phospholipases (PLPs), lipoxygenases (LOXs), chitinases (CHIA) and pectate lyase (PL), advocating that higher expression of these genes under stress conditions provide more membrane stability and protection to the tolerant genotype compared to the sensitive counterpart. During osmotic stress, PLPs and LOX can induce jasmonic acid (JA)-mediated membrane protection to reduce membrane damage (Yang et al. 2021). Moreover, hub genes like peroxiredoxin (PER1) and ethylene-insensitive protein 3 (EIN3/EIL1) are also involved in drought tolerance. Peroxiredoxin detoxifies reactive oxygen species (ROS) that accumulate during DS, helping to maintain cellular redox homoeostasis (Bhatt and Tripathi 2011; Dietz 2014). EIN3 is a key TF that regulates ethylene-responsive genes and is involved in modulating plant oxidative stress under drought conditions (Cui et al. 2015). In addition, the metabolomic analysis shows that AA metabolism, ALA metabolism and lysine degradation pathways are enriched in the cluster 4 (Figure 6B). Reports showed that under DS, the metabolic pathways of AA, ALA and lysine degradation play vital roles in plant tolerance. While AA is less common in plants, when present, it generates oxylipins, signalling molecules that help regulate drought-responsive genes and protect cellular membranes, enhancing structural stability under water-limiting conditions (Blée. 2002; Feussner and Wasternack 2002). ALA metabolism is pivotal for JA synthesis, where the LOX pathway converts ALA to JA, triggering drought-adaptive responses such as stomatal regulation, osmotic balance and antioxidant activity to mitigate oxidative stress (Wasternack and Hause 2013). Meanwhile, lysine degradation provides acetyl-CoA for the TCA cycle, supplying energy when photosynthesis is limited. It also yields glutamate, a precursor for proline, an osmoprotectant that aids in osmotic adjustments and ROS scavenging. Additionally, lysine catabolism feeds into the GABA shunt, further supporting cellular redox balance and oxidative damage prevention (Galili et al. 2001; Szabados and Savouré 2010). Together, these pathways allow plants to respond dynamically to DS by enhancing energy production, structural resilience and protective metabolite synthesis. All these findings suggest that the mechanisms of tolerance and membrane stabilization in the tolerant genotype prevent dhurrin from being released into the cytoplasm. Drought suppresses the cyanoamino acid metabolic pathway, reducing HCNp. In contrast, drought-mediated membrane damage leads to leakage of stored dhurrin from vacuoles into the cytoplasm, which might activate cyanoamino acid metabolism genes and defence response in the sensitive genotype (Figure 8).

5 | Conclusion

Sorghum stress-induced cyanogenesis can be highly complex and impacted by various variables, including the cultivar and the degree and duration of DS. The current study illustrates the transcriptomic and metabolomic differences between these genotypes, which exhibit variations in HCN/dhurrin accumulations and drought tolerance. Furthermore, the TF regulatory network and WGCNA analysis demonstrated that the drought-sensitive genotype's defence response and cyanoamino acid metabolism are activated when drought-induced membrane damages result in the continual release of dhurrin into the

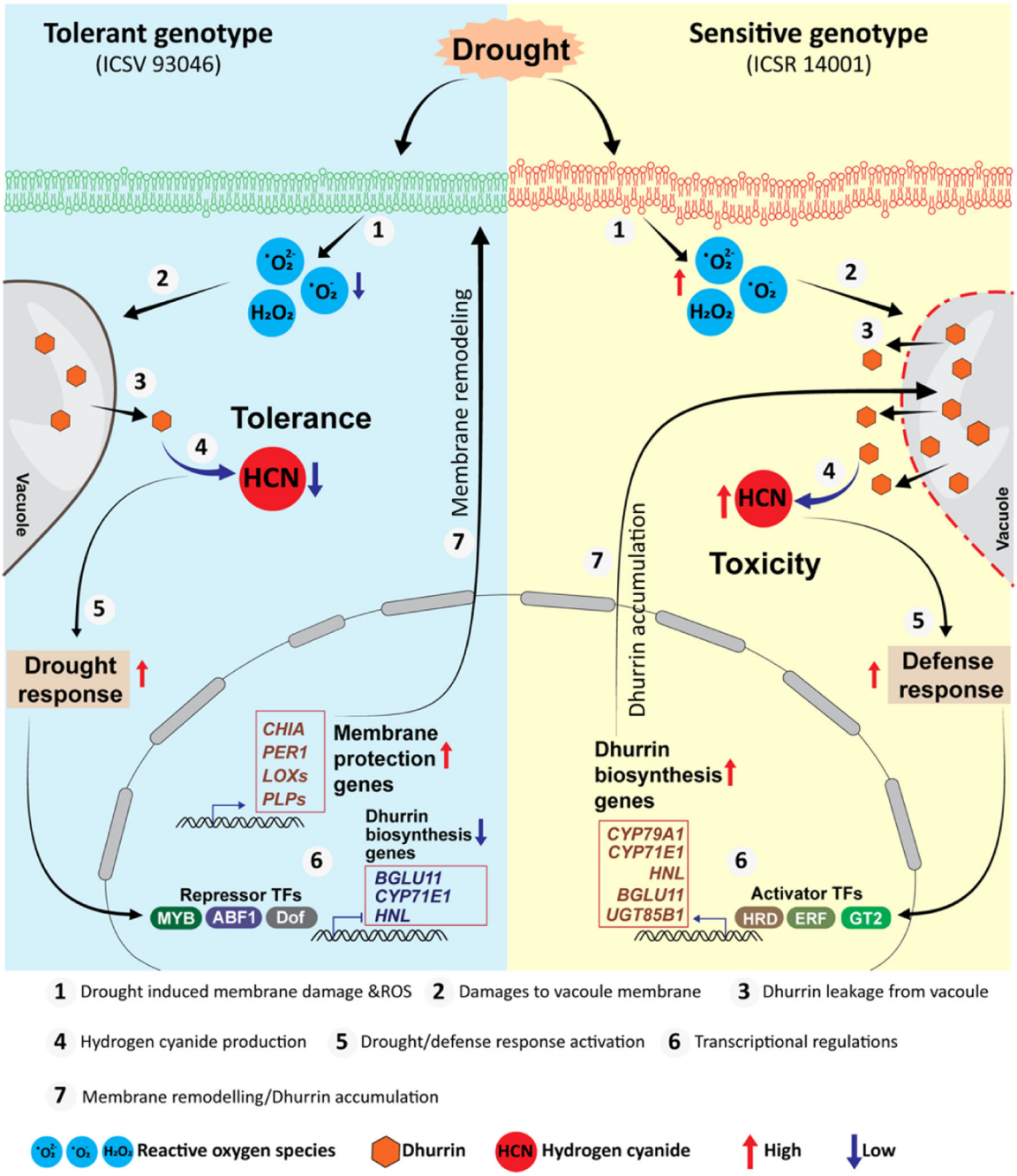

FIGURE 8 | Predicted mechanisms behind drought-induced hydrogen cyanide (HCN) induction in *Sorghum bicolor* genotypes. Under drought stress, reactive oxygen species (ROS) induced by stress damage cellular structures, including vacuole membranes. In the sensitive genotype, this damage leads to the release of dhurrin from vacuoles into the cytoplasm, where dhurrin converts to HCN, activating the defence response. This response triggers transcription factors (TFs) that promote the transcription of genes involved in dhurrin biosynthesis, resulting in increased production of dhurrin, which raises HCN levels and toxicity. Activating cell membrane protection genes in the tolerant genotype reduces these stress-induced membrane damages. Furthermore, drought-responsive TFs suppress the expression of dhurrin biosynthesis genes, lowering HCN levels under drought conditions and enhancing tolerance. [Color figure can be viewed at wileyonlinelibrary.com]

cytoplasm. On the other hand, under DS, the tolerant genotype's protection machinery, membrane remodelling and cell structure protection stop dhurrin from releasing continuously, which lowers the induction of HCN. The TF-network analysis predictions also support our hypothesis that drought-induced TFs reduced the expression of cyanoamino acid metabolism genes in tolerant genotypes. In contrast, ERF family TFs positively regulate these biosynthetic genes in sensitive genotypes. Differential expression of cyanoamino acid metabolism genes between the genotypes also supports our hypothesis. These observations summarize that DS may not be a direct inducer of cyanogenesis in sorghum; it can influence the levels of cyanogenic glucosides in the plant based on the severity of cellular damage caused. This study offers a novel perspective of dissecting the molecular mechanism and network of TFs and genes involved in the HCN induction pathways under DS. The

precise integration and dissection of physiological and molecular approaches in this study suggest possible candidate genes that can be validated in the future. Validation of these potential candidates might provide the mechanistic level of drought-induced HCN accumulation on sorghum. The genes identified from the study could be deployed into new breeding techniques like CRISPR-Cas9 and may aid in developing the reduced cyanogen or acyanogenic sorghum lines. This would greatly benefit the nutritional aspects of sorghum by improving the livestock feed, thereby increasing the forage sorghum production.

Acknowledgements

We thank ICRISAT, the sorghum breeding unit for the sorghum breeding lines, and the International Livestock Research Institute (ILRI) for their instrumental facility support. We would also like to thank Mallayee Srikanth and Bramhananda Reddy from ICRISAT for their help in conducting the glasshouse experiments. J.J. acknowledges the Council of Scientific and Industrial Research (CSIR), Government of India, for the PhD fellowship. P.S. acknowledges the financial support from the Department of Science and Technology, New Delhi, Government of India, for the support from the core grant research (CRG) grant file no. DST No: CRG/2019/004305. The contributions from J.K. are acknowledged and supported by the internal grant agency of the Faculty of Economics and Management, Czech University of Life Sciences, Prague, Czech Republic, grant number 2023B0005. This study was undertaken as part of the CGIAR Research Program on Grain Legumes and Dryland Cereals (CRP-GLDC), partially supported by CGIAR Fund Donors.

Conflicts of Interest

The authors declare no conflicts of interest.

Data Availability Statement

Raw sequence reads of RNA sequencing data are available in the NCBI SRA under accession number PRJNA1091444.

References

Abhilasha, A., and S. Roy Choudhury. 2021. "Molecular and Physiological Perspectives of Abscisic Acid Mediated Drought Adjustment Strategies." *Plants* 10, no. 12: 2769. https://doi.org/10.3390/plants10122769.

Al-Beiruty, R. A., S. H. Cheyed, and M. H. Hashim. 2020. "Hazards of Toxic Hydrocyanic Acid (HCN) in Sorghum and Ways to Control It: A Review." *Plant Archives* 20, no. 1: 2726–2731.

Ananda, G. K. S., S. L. Norton, C. Blomstedt, et al. 2022. "Transcript Profiles of Wild and Domesticated Sorghum Under Water-Stressed Conditions and the Differential Impact on Dhurrin Metabolism." *Planta* 255, no. 2: 51.

Andrews, S. 2010. "FastQC: A Quality Control Tool for High Throughput Sequence Data." http://www.bioinformatics.babraham.ac.uk/projects/fastqc.

Bak, S., R. Alice Kahn, H. Linde Nielsen, B. Lindberg Møller, and B. Ann Halkier. 1998. "Cloning of Three A-Type Cytochromes P450, CYP71E1, CYP98, and CYP99 From *Sorghum bicolor* (L.) Moench by a PCR Approach and Identification by Expression in *Escherichia coli* of CYP71E1 as a Multifunctional Cytochrome P450 in the Biosynthesis of the Cyanogenic Glucoside Dhurrin." *Plant Molecular Biology* 36: 393–405.

Bak, S., S. M. Paquette, M. Morant, et al. 2006. "Cyanogenic Glycosides: A Case Study for Evolution and Application of Cytochromes P450." *Phytochemistry Reviews* 5: 309–329.

Bhatt, I., and B. N. Tripathi. 2011. "Plant Peroxiredoxins: Catalytic Mechanisms, Functional Significance and Future Perspectives." *Biotechnology Advances* 29: 850–859.

Binder, S. 2010. "Branched-Chain Amino Acid Metabolism in *Arabidopsis thaliana*." *Arabidopsis Book* 8: e0137. https://doi.org/10.1199/tab.0137.

Blée, E. 2002. "Impact of Phyto-Oxylipins in Plant Defense." *Trends in Plant Science* 7: 315–322.

Blomstedt, C. K., R. M. Gleadow, N. O'Donnell, et al. 2012. "A Combined Biochemical Screen and TILLING Approach Identifies Mutations in *Sorghum bicolor* L. Moench Resulting in Acyanogenic Forage Production." *Plant Biotechnology Journal* 10, no. 1: 54–66. https://doi.org/10.1111/j.1467-7652.2011.00646.x.

Blomstedt, C. K., N. H. O'Donnell, N. Bjarnholt, et al. 2016. "Metabolic Consequences of Knocking Out UGT85B1, the Gene Encoding the Glucosyltransferase Required for Synthesis of Dhurrin in *Sorghum bicolor* (L. Moench)." *Plant and Cell Physiology* 57: 373–386.

Bohnert, H. J., D. E. Nelson, and R. G. Jensen. 1995. "Adaptations to Environmental Stresses." *Plant Cell* 7, no. 7: 1099.

Bolger, A. M., M. Lohse, and B. Usadel. 2014. "Trimmomatic: A Flexible Trimmer for Illumina Sequence Data." *Bioinformatics* 30: 2114–2120.

Van den Broeck, L., M. Dubois, M. Vermeersch, V. Storme, M. Matsui, and D. Inzé. 2017. "From Network to Phenotype: The Dynamic Wiring of an Arabidopsis Transcriptional Network Induced by Osmotic Stress." *Molecular Systems Biology* 13, no. 12: 961.

Busk, P. K., and B. L. Møller. 2002. "Dhurrin Synthesis in Sorghum Is Regulated at the Transcriptional Level and Induced by Nitrogen Fertilization in Older Plants." *Plant Physiology* 129: 1222–1231.

Calviño, M., J. M. Messing, and J. Messing. 2012. "Sweet Sorghum as a Model System for Bioenergy Crops." *Current Opinion in Biotechnology* 23: 323–329.

Chen, C., H. Chen, Y. Zhang, et al. 2020. "TBtools: An Integrative Toolkit Developed for Interactive Analyses of Big Biological Data." *Molecular Plant* 13: 1194–1202.

Chen, P., M. Yan, L. Li, et al. 2020. "The Apple DNA-Binding One Zinc-Finger Protein MdDof54 Promotes Drought Resistance." *Horticulture Research* 7: 195. https://doi.org/10.1038/s41438-020-00419-5.

Choi, J. W., H. H. Choi, Y. S. Park, M. J. Jang, and S. Kim. 2023. "Comparative and Expression Analyses of AP2/ERF Genes Reveal Copy Number Expansion and Potential Functions of ERF Genes in Solanaceae." *BMC Plant Biology* 23, no. 1: 48.

Choudhary, S., V. Vadez, C. Tom Hash, and P. B. Kavi Kishor. 2019. "Pearl Millet Mapping Population Parents: Performance and Selection Under Salt Stress Across Environments Varying in Evaporative Demand." *Proceedings of the National Academy of Sciences, India, Section B: Biological Sciences* 89: 201–211.

Conn, E. E. 1980. "Cyanogenic Compounds." *Annual Review of Plant Physiology* 31, no. 1: 433–451.

Cornara, L., J. Xiao, and B. Burlando. 2016. "Therapeutic Potential of Temperate Forage Legumes: A Review." *Critical Reviews in Food Science and Nutrition* 56: S149–S161.

Corrales, A. R., S. G. Nebauer, L. Carrillo, et al. 2014. "Characterization of Tomato Cycling Dof Factors Reveals Conserved and New Functions in the Control of Flowering." *Journal of Experimental Botany* 65: 995–1012.

Cowan, M. F., C. K. Blomstedt, S. L. Norton, R. J. Henry, B. L. Møller, and R. Gleadow. 2020. "Crop Wild Relatives as a Genetic Resource for Generating Low-Cyanide, Drought-Tolerant Sorghum." *Environmental and Experimental Botany* 169: 103884.

Cui, H., K. Tsuda, and J. E. Parker. 2015. "Effector-Triggered Immunity: From Pathogen Perception to Robust Defense." *Annual Review of Plant Biology* 66: 487–511.

Darbani, B., M. S. Motawia, C. E. Olsen, H. H. Nour-Eldin, B. L. Møller, and F. Rook. 2016. "The Biosynthetic Gene Cluster for the Cyanogenic Glucoside Dhurrin in *Sorghum bicolor* Contains Its Co-Expressed Vacuolar MATE Transporter." *Scientific Reports* 6: 37079.

Dietz, K.-J. 2014. "Redox Regulation of Transcription Factors in Plant Stress Acclimation and Development." *Antioxidants & Redox Signaling* 21: 1356–1372.

Djanaguiraman, M., S. Gowsiga, M. Govindaraj, et al. 2024. "Impact of Root Architecture and Transpiration Rate on Drought Tolerance in Stay-Green Sorghum." *Crop Science* 64: 2612–2629. https://doi.org/10.1002/csc2.21108.

Dubos, C., R. Stracke, E. Grotewold, B. Weisshaar, C. Martin, and L. Lepiniec. 2010. "MYB Transcription Factors in Arabidopsis." *Trends in Plant Science* 15: 573–581.

Dugas, D. V., M. K. Monaco, A. Olson, et al. 2011. "Functional Annotation of the Transcriptome of *Sorghum bicolor* in Response to Osmotic Stress and Abscisic Acid." *BMC Genomics* 12: 514. https://doi.org/10.1186/1471-2164-12-514.

Duncan, R. R. 1996. "Breeding and Improvement of Forage Sorghums for the Tropics." *Advances in Agronomy* 57: 161–185.

ElBasyoni, I., M. Saadalla, S. Baenziger, H. Bockelman, and S. Morsy. 2017. "Cell Membrane Stability and Association Mapping for Drought and Heat Tolerance in a Worldwide Wheat Collection." *Sustainability* 9: 1606.

Fan, X. L., and Y. K. Li. 2001. *Effect of Drought Stress and Drought Tolerance Heredity on Nitrogen Efficiency of Winter Wheat*. Springer Netherlands. https://doi.org/10.1007/0-306-47624-x_29.

FAOSTAT. 2018. *FAOSTAT Database*. http://faostat.fao.org.

Feussner, I., and C. Wasternack. 2002. "The Lipoxygenase Pathway." *Annual Review of Plant Biology* 53: 275–297.

Gakière, B., A. R. Fernie, and P. Pétriacq. 2018. "More to NAD^+ Than Meets the Eye: A Regulator of Metabolic Pools and Gene Expression in Arabidopsis." *Free Radical Biology and Medicine* 122: 86–95. https://doi.org/10.1016/j.freeradbiomed.2018.01.003.

Galili, G., G. Tang, X. Zhu, and B. Gakiere. 2001. "Lysine Catabolism: A Stress and Development Super-Regulated Metabolic Pathway." *Current Opinion in Plant Biology* 4: 261–266.

Gholipoor, M., S. Choudhary, T. R. Sinclair, C. D. Messina, and M. Cooper. 2013. "Transpiration Response of Maize Hybrids to Atmospheric Vapour Pressure Deficit." *Journal of Agronomy and Crop Science* 199: 155–160.

Gleadow, R. M., and B. L. Møller. 2014. "Cyanogenic Glycosides: Synthesis, Physiology, and Phenotypic Plasticity." *Annual Review of Plant Biology* 65: 155–185.

Gleadow, R. M., M. J. Ottman, B. A. Kimball, et al. 2016. "Drought-Induced Changes in Nitrogen Partitioning Between Cyanide and Nitrate in Leaves and Stems of Sorghum Grown at Elevated CO_2 Are Age Dependent." *Field Crops Research* 185: 97–102.

Gleadow, R. M., and I. E. Woodrow. 2002. "Mini-Review: Constraints on Effectiveness of Cyanogenic Glycosides in Herbivore Defense." *Journal of Chemical Ecology* 28: 1301–1313.

Hayes, C. M., B. D. Weers, M. Thakran, et al. 2016. "Discovery of a Dhurrin QTL in Sorghum: Co-Localization of Dhurrin Biosynthesis and a Novel Stay-Green QTL." *Crop Science* 56: 104–112.

Heraud, P., M. F. Cowan, K. M. Marzec, B. L. Møller, C. K. Blomstedt, and R. Gleadow. 2018. "Label-Free Raman Hyperspectral Imaging Analysis Localizes the Cyanogenic Glucoside Dhurrin to the Cytoplasm in Sorghum Cells." *Scientific Reports* 8: 2691.

Hoang, D. T., T. Hiroo, and K. Yoshinobu. 2018. "Nitrogen Use Efficiency and Drought Tolerant Ability of Various Sugarcane Varieties Under Drought Stress at Early Growth Stage." *Plant Production Science* 22, no. 2: 250–261. https://doi.org/10.1080/1343943x.2018.1540277.

Hogg, P. G., and H. L. Ahlgren. 1942. "A Rapid Method for Determining Hydrocyanic Acid Content of Single Plants of Sudan Grass." *Agronomy Journal* 34: 199–200.

Hösel, W., J. Berlin, T. N. Hanzlik, and E. E. Conn. 1985. "In-Vitro Biosynthesis of 1-(4′-Hydroxyphenyl)-2-Nitroethane and Production of Cyanogenic Compounds in Osmotically Stressed Cell Suspension Cultures of Eschscholtzia Californica Cham." *Planta* 166: 176–181.

Jadav, C. N., R. B. Makwana, S. S. Parikh, P. M. Gamit, K. S. Murthy, and P. U. Gajabhiye. 2019. "Hydrocyanic Acid (HCN) Estimation During Different Stages of Growth in Gundrijowar (*Sorghum vulgare*) Fodder Crop." *International Journal of Current Microbiology and Applied Sciences* 8: 1328–1333.

Jones, D. A. 1998. "Why Are so Many Food Plants Cyanogenic?" *Phytochemistry* 47: 155–162.

Jørgensen, M. E., D. Xu, C. Crocoll, et al. 2017. "Origin and Evolution of Transporter Substrate Specificity Within the NPF Family." *eLife* 6: e19466.

Kahn, R. A., S. Bak, I. Svendsen, B. A. Halkier, and B. L. Moller. 1997. "Isolation and Reconstitution of Cytochrome P450ox and In Vitro Reconstitution of the Entire Biosynthetic Pathway of the Cyanogenic Glucoside Dhurrin From Sorghum." *Plant Physiology* 115, no. 4: 1661–1670.

Kahn, R. A., T. Fahrendorf, B. A. Halkier, and B. L. Møller. 1999. "Substrate Specificity of the Cytochrome P450 Enzymes CYP79A1 and CYP71E1 Involved in the Biosynthesis of the Cyanogenic Glucoside Dhurrin in *Sorghum bicolor* (L.) Moench." *Archives of Biochemistry and Biophysics* 363: 9–18.

Karthika, G., J. Kholova, S. Alimagham, et al. 2019. "Measurement of Transpiration Restriction Under High Vapor Pressure Deficit for Sorghum Mapping Population Parents." *Plant Physiology Reports* 24: 74–85.

Karthika, N., and R. Kalpana. 2017. "Chemical Science Review and Letters HCN Content and Forage Yield of Multi-Cut Forage Sorghum Under Different Organic Manures and Nitrogen Levels." *Chemical Science Review and Letters* 6: 1659–1663.

Karthikeyan, B. J., C. Babu, A. J. Joel, and S. Ganeshram. 2015. "Development of a Reference Set of Sorghum (Sorghum spp.) for Cyanogenic Potential (HCN-p) and Evaluating Their Fodder Yield Traits." In *The XXIII International Grassland Congress (Sustainable use of Grassland Resour assland Resources for Forage Production, Biodiversity and Environmental Protection) Took Place in New Delhi, India From November 20 Through November 24, 2015*. Range Management Society of India.

Katamreddy, S. C., B. P. Reddy, P. B. K. Kishor, A. A. Kumar, and P. S. Reddy. 2024. "Identification and Expression Profile of Dhurrin Biosynthesis Pathway Genes in Sorghum Vegetative Tissues." *Plant Biotechnology Reports* 18: 195–205.

Katiyar, A., S. Smita, S. K. Lenka, R. Rajwanshi, V. Chinnusamy, and K. C. Bansal. 2012. "Genome-Wide Classification and Expression Analysis of MYB Transcription Factor Families in Rice and Arabidopsis." *BMC Genomics* 13: 544.

Katta, M. A. V. S. K., A. W. Khan, D. Doddamani, M. Thudi, and R. K. Varshney. 2015. "NGS-QCbox and Raspberry for Parallel, Automated and Rapid Quality Control Analysis of Large-Scale Next Generation Sequencing (Illumina) Data." *PLoS One* 10: e0139868.

Kholová, J., C. T. Hash, P. L. Kumar, R. S. Yadav, M. Kočová, and V. Vadez. 2010. "Terminal Drought-Tolerant Pearl Millet [*Pennisetum glaucum* (L.) R. Br.] Have High Leaf Aba and Limit Transpiration at High Vapour Pressure Deficit." *Journal of Experimental Botany* 61: 1431–1440.

Kim, D., B. Langmead, and S. L. Salzberg. 2015. "HISAT: A Fast Spliced Aligner With Low Memory Requirements." *Nature Methods* 12: 357–360.

Kitainda, V., and J. M. Jez. 2021. "Structural Studies of Aliphatic Glucosinolate Chain-Elongation Enzymes." *Antioxidants* 10, no. 9: 1500. https://doi.org/10.3390/antiox10091500.

Knudsen, C., K. Bavishi, and K. M. Viborg. 2020. "Stabilization of Dhurrin Biosynthetic Ezymes From Sorghum Bicolor Using a Natural Deep Eutectic Solvent." *Phytochemistry* 170: 112214. https://doi.org/10.1016/j.phytochem.2019.112214.

Knudsen, C., N. J. Gallage, C. C. Hansen, B. L. Møller, and T. Laursen. 2018. "Dynamic Metabolic Solutions to the Sessile Life Style of Plants." *Natural Product Reports* 35: 1140–1155.

Krasuska, U., K. Ciacka, P. Staszek, M. Tyminski, A. Wal, and A. Gniazdowska. 2023. "Hormetic Action of Cyanide: Plant Gasotransmitter and Poison." *Phytochemistry Reviews* 23, no. 3: 705–719. https://doi.org/10.1007/s11101-023-09904-w.

Liao, Y., G. K. Smyth, and W. Shi. 2014. "Featurecounts: An Efficient General Purpose Program for Assigning Sequence Reads to Genomic Features." *Bioinformatics* 30: 923–930.

Liu, H., J. Wang, J. Liu, T. Liu, and S. Xue. 2021. "Hydrogen Sulfide (H2S) Signaling in Plant Development and Stress Responses." *Abiotech* 2: 32–63.

Livak, K. J., and T. D. Schmittgen. 2001. "Analysis of Relative Gene Expression Data Using Real-Time Quantitative PCR and the 2−ΔΔCT Method." *Methods* 25: 402–408.

Lu, J., H. Ju, G. Zhou, et al. 2011. "An EAR-Motif-Containing ERF Transcription Factor Affects Herbivore-Induced Signaling, Defense and Resistance in Rice." *Plant Journal* 68: 583–596.

McCarthy, R. L., R. Zhong, S. Fowler, et al. 2010. "The Poplar MYB Transcription Factors, PtrMYB3 and PtrMYB20, Are Involved in the Regulation of Secondary Wall Biosynthesis." *Plant and Cell Physiology* 51: 1084–1090.

Meng, X., and S. Zhang. 2013. "MAPK Cascades in Plant Disease Resistance Signaling." *Annual Review of Phytopathology* 51: 245–266.

Morant, A. V., K. Jørgensen, B. Jørgensen, et al. 2007. "Lessons Learned From Metabolic Engineering of Cyanogenic Glucosides." *Metabolomics* 3: 383–398.

Møller, B. L. 2010. "Functional Diversifications of Cyanogenic Glucosides." *Current Opinion in Plant Biology* 13: 337–346.

Møller, B. L., and T. Laursen. 2021. "Metabolons and Bio-Condensates: The Essence of Plant Plasticity and the Key Elements in Development of Green Production Systems." *Advances in Botanical Research* 97: 185–223.

Neilson, E. H., A. M. Edwards, C. K. Blomstedt, B. Berger, B. L. Møller, and R. M. Gleadow. 2015. "Utilization of a High-Throughput Shoot Imaging System to Examine the Dynamic Phenotypic Responses of a C4 Cereal Crop Plant to Nitrogen and Water Deficiency Over Time." *Journal of Experimental Botany* 66, no. 7: 1817–1832.

O'Donnell, N. H., B. L. Møller, A. D. Neale, J. D. Hamill, C. K. Blomstedt, and R. M. Gleadow. 2013. "Effects of PEG-Induced Osmotic Stress on Growth and Dhurrin Levels of Forage Sorghum." *Plant Physiology and Biochemistry* 73: 83–92.

Osakabe, Y., K. Yamaguchi-Shinozaki, K. Shinozaki, and L. S. P. Tran. 2013. "Sensing the Environment: Key Roles of Membrane-Localized Kinases in Plant Perception and Response to Abiotic Stress." *Journal of Experimental Botany* 64: 445–458.

Pahuja, S., S. Arya, S. Kumari, and R. Panchta. 2014. "Evaluation of Forage Sorghum Hybrids [*Sorghum bicolor* (L.) Moench]." *Forage Research* 40, no. 3: 159–162.

Pandey, A. K., P. Madhu, and B. V. Bhat. 2019. "Down-Regulation of CYP79A1 Gene Through Antisense Approach Reduced the Cyanogenic Glycoside Dhurrin in [*Sorghum bicolor* (L.) Moench] to Improve Fodder Quality." *Frontiers in Nutrition* 6: 122.

Pinto, A. P., A. De Varennes, M. L. S. Gonçalves, and A. M. Mota. 2006. "Sorghum Detoxification Mechanisms." *Journal of Plant Nutrition* 29, no. 7: 1229–1242. https://doi.org/10.1080/01904160600767450.

Pičmanová, M., E. H. Neilson, M. S. Motawia, et al. 2015. "A Recycling Pathway for Cyanogenic Glycosides Evidenced by the Comparative Metabolic Profiling in Three Cyanogenic Plant Species." *Biochemical Journal* 469: 375–389.

Pluskal, T., S. Castillo, A. Villar-Briones, and M. Orešič. 2010. "MZmine 2: Modular Framework for Processing, Visualizing, and Analyzing Mass Spectrometry-Based Molecular Profile Data." *BMC Bioinformatics* 11: 395.

Prasanth, A., A. Premnath, and R. Muthurajan. 2021. "Genetic Divergence Study for Duration and Biomass Traits in Sorghum [*Sorghum bicolor* (L.) Moench]." *Electronic Journal of Plant Breeding* 12: 22–27.

Qu, X., J. Zou, J. Wang, K. Yang, X. Wang, and J. Le. 2022. "A Rice R2R3-Type MYB Transcription Factor OsFLP Positively Regulates Drought Stress Response via OsNAC." *International Journal of Molecular Sciences* 23, no. 11: 5873. https://doi.org/10.3390/ijms23115873.

Rezaul Haque, M., and J. Howard Bradbury. 2002. "Total Cyanide Determination of Plants and Foods Using the Picrate and Acid Hydrolysis Methods." *Food Chemistry* 77, no. 1: 107–114.

Saunders, J. A., and E. E. Conn. 1978. "Presence of the Cyanogenic Glucoside Dhurrin in Isolated Vacuoles Fromsorghum." *Plant Physiology* 61: 154–157.

Selmar, D., and M. Kleinwächter. 2013. "Stress Enhances the Synthesis of Secondary Plant Products: The Impact of Stress-Related Over-Reduction on the Accumulation of Natural Products." *Plant and Cell Physiology* 54: 817–826.

Seo, P. J., S. B. Lee, M. C. Suh, M.-J. Park, Y. S. Go, and C. M. Park. 2011. "The MYB96 Transcription Factor Regulates Cuticular Wax Biosynthesis Under Drought Conditions in Arabidopsis." *Plant Cell* 23, no. 3: 1138–1152. https://doi.org/10.1105/tpc.111.083485.

Sharmin, R. A., M. R. Bhuiyan, W. Lv, et al. 2020. "RNA-Seq Based Transcriptomic Analysis Revealed Genes Associated With Seed-Flooding Tolerance in Wild Soybean (Glycine soja Sieb. & Zucc." *Environmental and Experimental Botany* 171: 103906.

Shekoofa, A., and T. R. Sinclair. 2018. "Aquaporin Activity to Improve Crop Drought Tolerance." *Cells* 7: 123.

Sinclair, T. R., G. L. Hammer, and E. J. Van Oosterom. 2005. "Potential Yield and Water-Use Efficiency Benefits in Sorghum From Limited Maximum Transpiration Rate." *Functional Plant Biology* 32: 945–952.

Sivasakthi, K., E. Marques, N. Kalungwana, et al. 2019. "Functional Dissection of the Chickpea (*Cicer arietinum* L.) Stay-Green Phenotype Associated With Molecular Variation at an Ortholog of Mendel's I Gene for Cotyledon Color: Implications for Crop Production and Carotenoid Biofortification." *International Journal of Molecular Sciences* 20: 5562.

Sudhakar Reddy, P., D. Srinivas Reddy, K. Sivasakthi, P. Bhatnagar-Mathur, V. Vadez, and K. K. Sharma. 2016. "Evaluation of Sorghum [*Sorghum bicolor* (L.)] Reference Genes in Various Tissues and Under Abiotic Stress Conditions for Quantitative Real-Time PCR Data Normalization." *Frontiers in Plant Science* 7: 529.

Szabados, L., and A. Savouré. 2010. "Proline: A Multifunctional Amino Acid." *Trends in Plant Science* 15: 89–97.

Takafuji, K., H. Rim, K. Kawauchi, et al. 2020. "Evidence That ERF Transcriptional Regulators Serve as Possible Key Molecules for Natural Variation in Defense Against Herbivores in Tall Goldenrod." *Scientific Reports* 10: 5352.

Takos, A. M., C. Knudsen, D. Lai, et al. 2011. "Genomic Clustering of Cyanogenic Glucoside Biosynthetic Genes Aids Their Identification in Lotus Japonicus and Suggests the Repeated Evolution of This Chemical Defence Pathway." *Plant Journal* 68: 273–286.

Tattersall, D. B., S. Bak, P. R. Jones, et al. 2001. "Resistance to an Herbivore Through Engineered Cyanogenic Glucoside Synthesis." *Science* 293: 1826–1828.

Terler, G., R. Resch, S. Gappmaier, and L. Gruber. 2021. "Nutritive Value for Ruminants of Different Fresh and Ensiled Sorghum (*Sorghum bicolor* [L.] Moench) Varieties Harvested at Varying Maturity Stages." *Archives of Animal Nutrition* 75: 167–182.

Thorsøe, K. S., S. Bak, C. E. Olsen, A. Imberty, C. Breton, and B. Lindberg Møller. 2005. "Determination of Catalytic Key Amino Acids and UDP Sugar Donor Specificity of the Cyanohydrin Glycosyltransferase UGT85B1 From *Sorghum bicolor*. Molecular Modeling Substantiated by Site-Specific Mutagenesis and Biochemical Analyses." *Plant Physiology* 139: 664–673.

Vadez, V., A. Grondin, K. Chenu, et al. 2024. "Crop Traits and Production Under Drought." *Nature Reviews Earth & Environment* 5: 211–225. https://doi.org/10.1038/s43017-023-00514-w.

De Vos, R. C., S. Moco, A. Lommen, J. J. Keurentjes, R. J. Bino, and R. D. Hall. 2007. "Untargeted Large-Scale Plant Metabolomics Using Liquid Chromatography Coupled to Mass Spectrometry." *Nature Protocols* 2: 778–791.

Wasternack, C., and B. Hause, 2013. "An Update to the 2007 Review in Annals of Botany." *Annals of Botany* 111, no. 6: 1021–1058. https://doi.org/10.1093/aob/mct067.

Wei, Q., F. Zhang, G. He, et al. 2017. "A Wheat R2R3-Type MYB Transcription Factor TaODORANT1 Positively Regulates Drought and Salt Stress Responses in Transgenic Tobacco Plants." *Frontiers in Plant Science* 8, no. 1249721: 1374. https://doi.org/10.3389/fpls.2017.01374.

Wheeler, J., C. Mulcahy, J. Walcott, and G. Rapp. 1990. "Factors Affecting the Hydrogen Cyanide Potential of Forage Sorghum." *Australian Journal of Agricultural Research* 41: 1093–1100.

Wu, J., H. Gao, X. Zhu, and D. Li. 2020. "An ERF Transcription Factor Enhances Plant Resistance to *Myzus persicae* and *Spodoptera litura*." *Biotechnology & Biotechnological Equipment* 34: 946–954.

Yang, N., Y. Zhang, L. Chen, et al. 2021. "G Protein and PLD? are Involved in JA to Regulate Osmotic Stress Responses in Arabidopsis Thaliana." *Biochemistry and Biophysics Reports* 26: 100952. https://doi.org/10.1016/J.BBREP.2021.100952.

Yi, X., Z. Du, and Z. Su. 2013. "PlantGSEA: A Gene Set Enrichment Analysis Toolkit for Plant Community." *Nucleic Acids Research* 41: W98–W103.

Yu, Y., M. Yu, S. Zhang, et al. 2022. "Transcriptomic Identification of Wheat AP2/ERF Transcription Factors and Functional Characterization of TaERF-6-3A in Response to Drought and Salinity Stresses." *International Journal of Molecular Sciences* 23: 3272.

Zayed, B. A., H. A. Ghazy, M. E. Negm, et al. 2023. "Response of Varied Rice Genotypes on Cell Membrane Stability, Defense System, Physio-Morphological Traits and Yield Under Transplanting and Aerobic Cultivation." *Scientific Reports* 13, no. 1: 5765.

Zhang, S., Y. Hu, Y. Wang, et al. 2023. "Integrated Transcriptomics and Metabolomics Reveals That Regulating Biosynthesis and Metabolism of HCN and GABA Plays a Key Role in Drought Resistance of Wild Soybean." *Environmental and Experimental Botany* 215: 105505. https://doi.org/10.1016/j.envexpbot.2023.105505.

Supporting Information

Additional supporting information can be found online in the Supporting Information section.